BIOCHEMISTRY
including biophysical chemistry & molecular biology

Article

pubs.acs.org/biochemistry

Identification of Destabilizing and Stabilizing Mutations of Ste2p, a G Protein-Coupled Receptor in *Saccharomyces cerevisiae*

Jeffrey Zuber,[†] Shairy Azmy Danial,[†] Sara M. Connelly,[†] Fred Naider,[‡,§] and Mark E. Dumont*[,†]

[†]Department of Biochemistry and Biophysics, University of Rochester School of Medicine and Dentistry, P.O. Box 712, Rochester, New York 14642, United States

[‡]Department of Chemistry, College of Staten Island, and Macromolecular Assemblies Institute, City University of New York, New York, New York 10314, United States

Supporting Information

ABSTRACT: The isolation of mutations affecting the stabilities of transmembrane proteins is useful for enhancing the suitability of proteins for structural characterization and identification of determinants of membrane protein stability. We have pursued a strategy for the identification of stabilized variants of the yeast α-factor receptor Ste2p. Because it was not possible to screen directly for mutations providing thermal stabilization, we first isolated a battery of destabilized temperature-sensitive variants, based on loss of signaling function and decreased levels of binding of the fluorescent ligand, and then screened for intragenic second-site suppressors of these phenotypes. The initial screens recovered singly and multiply substituted mutations conferring temperature sensitivity throughout the predicted transmembrane helices of the receptor. All of the singly substituted variants exhibit decreases in cell-surface expression. We then screened randomly mutagenized libraries of clones expressing temperature-sensitive variants for second-site suppressors that restore elevated levels of binding sites for fluorescent ligand. To determine whether any of these were global suppressors, and thus likely stabilizing mutations, they were combined with different temperature-sensitive mutations. Eight of the suppressors exhibited the ability to reverse the defect in ligand binding of multiple temperature-sensitive mutations. Combining certain suppressors into a single allele resulted in levels of suppression greater than that seen with either suppressor alone. Solubilized receptors containing suppressor mutations in the absence of temperature-sensitive mutations exhibit a reduced tendency to aggregate during immobilization on an affinity matrix. Several of the suppressors also exhibit allele-specific behavior indicative of specific intramolecular interactions in the receptor.

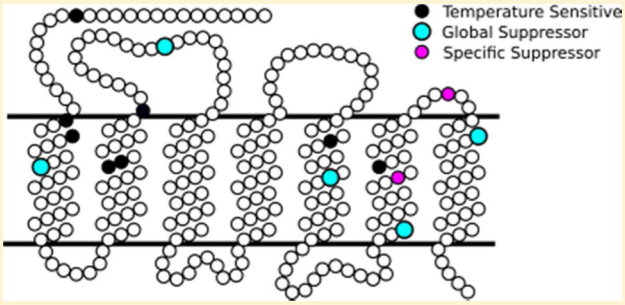

Transmembrane proteins (TMPs) are encoded by 20−30% of the open reading frames in most genomes,[1] play critical physiological roles in signaling, transmembrane transport, and catalysis, and are the targets of a large fraction of clinically useful drugs.[2] However, determination of the structures of TMPs, particularly of eukaryotic TMPs, remains challenging and such structures are grossly under-represented in the protein structure database.[3] Reasons for the difficulty in the determination of structures of TMPs include low levels of expression (in native and heterologous expression systems), the structure-perturbing effects of detergents used for the extraction and purification of TMPs, the need to establish intermolecular contacts involving both hydrophobic and hydrophilic surfaces, and the instability and flexibility of TMPs, which can hinder packing into well-ordered crystals (see ref 4).

The growing number of examples of successful structure determination of TMPs can be attributed, in part, to the implementation of strategies for stabilization of TMP folding. Strategies for stabilization also appear to be of particular importance in protecting the native conformations of TMPs against the denaturing effects of detergents used in their solubilization and purification.[5,6] However, our current understanding of the underlying basis of folding of transmembrane proteins is not sufficient to provide a reliable basis for rational design of amino acid substitutions that will provide TMP stabilization. Successful strategies for TMP stabilization have included the use of proteins derived from thermophilic organisms,[7] the use of TMP variants that contain an insertion of a stable soluble protein in place of a flexible loop or fused to the N-terminus of the protein,[8−38] the use of variant forms of TMPs containing point mutations that confer stability or conformational homogeneity,[24,39−45] and cocrystallization with anti-TMP antibodies.[16,17,46,47] These strategies, while providing important advances for structure determination, have been suboptimal in several respects. (1) Development of appropriate antibodies and strategies for copurification and cocrystallization is time-consuming, and antibody binding can, in some cases, perturb protein structures. (2) Thermophilic orthologs of

Received: October 20, 2014
Revised: February 3, 2015
Published: February 3, 2015

DOI: 10.1021/bi501314t
Biochemistry 2015, 54, 1787−1806

membrane proteins are not always available and may be difficult to express in common expression systems. (3) Fusion and truncation of membrane proteins can lead to substantial loss or alteration of the protein's function.[9] (4) Generation and assay of large numbers of individual site-directed mutations is time-consuming and allows sampling of only a limited subset of sequence space.

We report here the development of a protocol for the identification of stabilizing mutations in TMPs. The protocol is based on the use of fluorescence-activated cell sorting (FACS) to screen a library of randomly mutated TMPs expressed in yeast cells to identify variants with enhanced thermal stabilities. This approach is distinct from previous protocols for stabilization based on one-at-a-time testing of large numbers of site-directed substitutions[24,40−44] in that it provides more direct and complete screening of the full range of possible amino acid substitutions. However, related random screening approaches using bacterial expression systems have been successfully applied to the development of thermostabilized variants of a soluble protein[48] as well as several different examples of G protein-coupled receptors (GPCRs).[45,49−54]

Among TMPs, G protein-coupled receptors (GPCRs) make up an important class of receptors involved in the transduction of diverse extracellular signals. The first structure of a GPCR was obtained by crystallography of the native protein (rhodopsin) derived from native tissue,[55] but all subsequent crystal structures of other GPCRs have been acquired using heterologously expressed protein that has been modified to enhance stability and homogeneity. In many cases, this has resulted in loss[9] or modification of the signaling activity.[5,56] As a test system for implementation of the mutagenesis and screening approach, we have focused on the pheromone receptor Ste2p, a GPCR that is normally expressed in *Mat***a** haploid cells of the yeast *Saccharomyces cerevisiae*. Ste2p is activated by binding of α-factor, a 13-residue peptide secreted by cells of the opposite *Matα* mating type, resulting in G protein-dependent signaling via a MAP kinase cascade with downstream effects that include the transcriptional activation of a number of genes, as well as arrest of the cell cycle.[57] Although Ste2p exhibits very little sequence similarity to mammalian receptors, it activates a trimeric G protein that is closely related to trimeric mammalian G proteins. Furthermore, some mammalian GPCRs can activate the yeast mating pathway, indicating that yeast and mammalian GPCRs share similar mechanisms of action.[58−60] Purification of the Ste2p receptor has been reported by several groups.[61−63] Determination of the structure of Ste2p could allow identification of conserved structural elements that underlie signaling function across the range of widely diverged GPCR sequences. Moreover, techniques developed to identify stabilized Ste2p may be applied to mammalian GPCRs and other TMPs.

Initial experiments examining the stability of Ste2p indicated that the native protein, once it is incorporated into the plasma membrane of cells, is stable to temperatures well above those at which yeast can survive. Furthermore, we, and others,[64] have found that high-temperature treatment induces a transition in intact yeast cells that results in high levels of nonspecific binding of ligand that does not involve Ste2p receptors. These observations preclude the use of assays of binding of ligand to yeast cells for directly screening for receptor variants exhibiting enhanced thermal stability. Consequently, we have pursued an approach that involves initial identification of variant receptors with decreased thermal stability (temperature-sensitive receptors) followed by isolation of intragenic second-site suppressor mutations that suppress the initial temperature-sensitive alleles. Our goal was to identify "global suppressors" that provide overall stabilization of the protein rather than directly interacting with particular destabilizing mutations in the original temperature-sensitive alleles.[65] Such suppressor mutations are expected to provide enhanced stability when they are transferred from the temperature-sensitive background into otherwise wild-type receptors. Because a hallmark of "global suppression" is the ability to suppress diverse starting temperature-sensitive alleles, pursuit of this approach requires isolation of a collection of different temperature-sensitive starting alleles.

We describe herein the isolation of a collection of temperature-sensitive alleles of the gene encoding the yeast pheromone receptor Ste2p and the identification and characterization of intragenic second-site suppressors of these initial destabilizing mutations. Analysis of an array of combinations of temperature-sensitive and suppressor mutations confirmed the global nature of some of the suppressors but also provided evidence of certain allele-specific interactions between starting and suppressing mutations. When transferred to an otherwise normal receptor, some of the suppressor mutations enhanced the ability of the detergent-solubilized Ste2p receptor to survive initial stages of purification.

MATERIALS AND METHODS

Strains and Plasmids. The strains and plasmids used in this study are listed in Tables S1−S5 of the Supporting Information. All yeast strains used in this study were generated by transforming plasmids into the host strain A232 (*MATa ste2-Δ bar1⁻ cry1^R ade2-1 his4-580 lys2$_{oc}$ tyr1$_{oc}$ SUP4-3^{ts} leu2 ura3 FUS1::p[FUS1-lacZ TRP1]*), originally derived from strain DJ213-7-3.[67] Because strain A232 lacks the normal chromosomal copy of *STE2*, plasmid-borne alleles provide the only Ste2p in the cells.

Plasmids encoding full-length *STE2* were derived from plasmid pMD1483, which was constructed by ligating a SacI−SphI fragment of pMD240[66] containing *STE2* fused to a C-terminal triple-HA epitope into similarly digested pMD1383.[68] The plasmids encoding C-terminally truncated *STE2* were derived from plasmid pMD1422.[69] This is a multicopy plasmid encoding Ste2p truncated after amino acid 303, which is C-terminal to the end of the seventh transmembrane helix. A triple repeat of the c-myc epitope tag is fused to the C-terminal end of this truncated Ste2p. In some cases, temperature-sensitive mutations identified in the genetic screens were transferred from plasmids encoding full-length Ste2p into a plasmid encoding truncated Ste2p by digesting with SphI and KpnI and ligating the *STE2*-containing fragment into SphI−KpnI-cut pMD1422.

Mutagenesis. Site-directed mutagenesis was performed essentially as described previously.[70,71] Oligonucleotides used for site-directed mutagenesis and polymerase chain reaction (PCR) are listed in Table S6 of the Supporting Information. For the construction of double mutants, two oligonucleotides, each encoding a separate mutation, were used in a single reaction, with the exception of cases in which the two oligonucleotides would overlap, in which case a longer single oligonucleotide encoding both mutations was used.

Mutagenized libraries of full-length receptors were generated by error-prone PCR as described previously.[71,72] PCRs were performed with skewed dNTP ratios (0.2 mM dATP and

DOI: 10.1021/bi501314t
Biochemistry 2015, 54, 1787−1806

dGTP vs 1 mM dCTP and dTTP) and elevated Mg^{2+} and Mn^{2+} concentrations (7 and 0.5 mM, respectively) to introduce mutations into the PCR product. The 30 cycles of PCR were conducted with *Taq* DNA polymerase, 200 pM template, and primers ON915 and ON918 (300 nM each). The region amplified by error-prone PCR corresponded to residues 4−304 of Ste2p, covering the entire membrane-spanning region. The mutagenized PCR product was cotransformed into yeast with plasmid pMD1483 that had been doubly digested with HpaI and KpnI (which cut *STE2* at positions corresponding to amino acids V45 and G273). Homologous recombination during transformation recircularizes the plasmid with the mutagenized PCR product, resulting in the incorporation of random mutations into the plasmid-encoded *STE2*.

Mutagenized libraries of the truncated receptor were generated by mutagenic PCR using the Agilent Genemorph II random mutagenesis kit with 500 ng of template DNA per reaction. Twenty-five cycles of PCR were performed using primers ON915 and ON918. The coding region of the C-terminally truncated *STE2* gene encoding residues 4 to 303 was targeted for mutagenesis. As performed for construction of libraries of full-length receptors, the PCR product was transformed into yeast along with HpaI−KpnI doubly digested plasmid pMD1422, the ends of which overlapped the mutagenized PCR product by 126 bases on the 5′ side of *STE2* and 112 bases on the 3′ side. After transformation into yeast, plasmids were extracted from randomly selected colonies and sequenced to determine the mutation rate, which averaged 3.6 mutations per sequenced clone.

Screen for Temperature-Sensitive *STE2* Alleles Based on Loss of Pheromone-Dependent Growth Arrest. To identify clones expressing temperature-sensitive receptors, we developed a screen for receptors that lose signaling function at high temperatures, preventing α-factor-dependent growth arrest. Libraries of mutagenized plasmids encoding full-length *STE2* were transformed into *ste2*-Δ yeast strain A232. Freshly transformed cells were replica plated onto one set of plates that contained 300 nM α-factor and another set that lacked α-factor. One plate of each type was incubated at 24 °C and another at 34 °C. Cells from colonies that grew in the presence of α-factor at 34 °C but not at 24 °C were collected, streaked to single colonies, and then inoculated into liquid culture. Plasmids were isolated from yeast cells using a Wizard Miniprep Kit (Promega Corp.). Cells were disrupted by vortexing with zirconia beads (Biospec Products Inc.) in the lysis buffer from the kit. The lysate was centrifuged for 2 min at 100*g* to pellet the beads, and the supernatant was mixed with the kit's neutralization solution. All other steps (clearing the lysate, binding to resin, washing the resin, and elution of the DNA) followed the manufacturer's standard protocol.

Growth Arrest Assay. To perform the growth arrest assay, sets of plates were prepared by casting either 25 mL of medium in 90 mm round plates or 50 mL in 128 mm × 86 mm rectangular plates. After cooling, α-factor was spread on each plate to the desired concentration and equilibrated for at least 24 h. The strains to be tested were cultured to an OD_{600} of 1 in synthetic medium lacking α-factor and uracil (SD-ura) and then diluted with the same liquid medium to an OD_{600} of 0.3 in a 96-well plate. The cultures were then 10-fold serially diluted into neighboring wells. Two microliters from each dilution was spotted onto each plate containing different concentrations of α-factor, allowed to dry, incubated at the appropriate temperatures, and photographed after being grown for 2 days.

Flow Cytometry and Cell Sorting. The fluorescent ligand used in this project, [K^7(NBD),Nle^{12}]-α-factor, contains the fluorophore NBD (7-nitrobenz-2-oxa-1,3-diazol-4-yl) conjugated to the lysine at position 7 in α-factor. In addition, the methionine normally present at position 12 of α-factor is replaced by norleucine.[73] (Norleucine is isosteric to the native methionine residue that it replaces and does not affect biological activity or binding.) The fluorescent ligand has a measured K_D of ∼27 nM compared to a K_D of ∼8 nM for unlabeled α-factor.[73] The fluorescent ligand was also shown to be able to trigger growth arrest in exposed cells with an EC_{50} similar to that of unlabeled α-factor.[74]

Ligand binding assays were performed as previously reported.[74] The strains to be assayed were grown to an OD_{600} of ∼1 in SD-ura medium. Samples consisted of 1.5×10^6 cells and the relevant concentration of ligand in 20 mM sodium acetate (pH 4.6) in a final sample volume of 500 μL. Samples were maintained at 0 °C during and after addition of ligand to prevent endocytosis of receptors. The cellular fluorescence was analyzed using a BD FACSCanto flow cytometer. The fluorescent signal due to binding was calculated by subtracting the mean autofluorescence of a control without ligand from the mean fluorescence of the sample with ligand. Ligand binding parameters were determined by fitting the fluorescence measurements of samples that had been incubated with varying concentrations of fluorescent α-factor to a single-site binding equation that included a nonspecific binding component using the ligand-binding module of the nonlinear least-squares function of SigmaPlot (Systat Software Inc.). The listed binding parameters for variants of Ste2p represent the averages of independent fits of data from the three genetically independent yeast transformants. Because of day-to-day variability in the assay, strains expressing mutant alleles were always compared against strains expressing comparable wild-type alleles assayed in parallel.

For cell sorting, samples that contained cells cultured at the desired temperature and 300 nM [K^7(NBD),Nle^{12}]-α-factor in 20 mM acetate buffer (pH 4.6) were prepared. The two-stage screen for temperature-sensitive alleles was conducted using selection gates defined with reference to the fluorescence channel histogram to minimize the number of cells from the unmutagenized control and to maximize the number of events from the randomly mutagenized library (Figure S1 of the Supporting Information). The selected population was split evenly between two FACS sorting gates, with each sorting gate collecting 15% of the total population, as shown in Figure S1A of the Supporting Information. The pool of clones that had been selected for the highest levels of ligand binding after growth at 24 °C (P4 in Figure S1A) was cultured at 34 °C overnight and then subjected to a second screen that selected for cells with low levels of ligand binding (the lowest 30% of fluorescence) when cultured at the elevated temperature (P5 in Figure S1B of the Supporting Information). In the screens for suppressors, selection gates were chosen with reference to two-dimensional dot plots of fluorescence channel versus forward scatter, to minimize the number of cells from the unmutagenized control and to maximize the number of events from the randomly mutagenized library (Figure S2 of the Supporting Information). Because large cells are expected to bind more fluorescent ligand than small cells, and forward scatter in flow cytometry is related to the size of cells, a diagonal orientation of the selection gate was used to eliminate cells that exhibit high

DOI: 10.1021/bi501314t
Biochemistry 2015, 54, 1787−1806

fluorescence because they are large rather than because they express more stable receptors.

Preparation of Cell Lysates and Membrane Fractions. Tagged alleles of *STE2* were used in all experiments to allow immunoblotting with anti-tag antibodies. Full-length alleles of *STE2* consisted of fusions to three copies of the influenza HA epitope tag. C-terminally truncated alleles of *STE2* were fused to a triple c-myc epitope tag, as described previously.[75] For immunoblotting of cell lysates, strains were cultured in SD-ura to an OD_{600} of 1. Five OD × milliliters of culture (~1×10^8 cells) were pelleted by centrifugation at 14000*g* for 2 min and resuspended in 20 mM sodium acetate (pH 4.6) with 1 mM freshly prepared phenylmethanesulfonyl fluoride (PMSF) (from a 100 mM stock in ethanol). The cells were disrupted by adding zirconia beads (Biospec Products Inc.) and conducting 10 cycles of disruption for 20 sec by vortexing performed at 8 °C, interspersed with incubations for 1 min on ice.

To isolate membrane fractions, the cell lysates were centrifuged for 2 min at 4 °C and 200*g* to pellet the zirconia beads. Another 2 min spin at 200*g* further separated unbroken cells and cell wall fragments from the lysate. The supernatant from this spin was then centrifuged at 18000*g* for 45 min at 4 °C to pellet the cell membranes.

Membranes were solubilized by resuspending them in 1% *n*-dodecyl β-D-maltopyranoside (DDM) (Affymetrix). The samples were then nutated at room temperature for 2 h. To remove any unsolubilized fraction, the samples were centrifuged for 30 min at 4 °C and 18000*g*.

For immunoblotting, cell lysates, resuspended membrane fractions, or solubilized membranes were mixed with gel loading buffer [100 mM Tris (pH 6.8), 0.1 mM EDTA, 9 M urea, 5% SDS, and 0.02 mg/mL bromophenol blue] and then applied to Bio-Rad Criterion 8−15% Tris-HCl gels. Each well was loaded with the lysate prepared from 0.04 OD_{600} × milliliter of cells. After electrophoresis, the gels were transferred to 0.2 μm nitrocellulose membranes by overnight electroblotting. The membrane was blocked by incubation in 2.5% Carnation powdered milk for 2 h and then incubated for 2 h with a 1:5000 dilution of anti-HA antibody (Roche Inc.) or anti-c-myc antibody (Roche Inc.) followed by an additional 2 h incubation with a 1:15000 dilution of goat anti-mouse antibody conjugated to horseradish peroxidase. The membrane was then incubated with SuperSignal West Dura Chemiluminescent Substrate (Thermo Scientific), followed by imaging on CL-X Posure film (Thermo Scientific).

Immobilization of Solubilized Receptors. For immobilization of solubilized receptors, we used 8 μm polystyrene beads that were preconjugated to goat anti-mouse antibodies (Spherotech). The beads were washed with phosphate-buffered saline (pH 7.4) (PBS) and resuspended in fresh PBS. They were then incubated for 2 h at room temperature with agitation with mouse anti-myc antibodies (Roche Inc.) at a concentration of 20 μg of antibody/mL of beads. The beads were then washed with fresh PBS and incubated with solubilized receptor in PBS with 0.1% DDM and 1 mM PMSF with agitation for 2 h. After protein binding, the beads were pelleted by centrifugation and washed with PBS containing 0.1% DDM and 1 mM PMSF.

RESULTS

We report here the development of an approach for identifying mutations that enhance the thermal stability of the yeast α-factor receptor, Ste2p. The approach is based on the use of an assay for high-affinity binding of a cell-impermeant fluorescent ligand to monitor the abundance of correctly folded receptors at the cell surface.[74] However, this strategy could not be used directly to stabilize wild-type receptors because of the loss of yeast viability and the high level of nonspecific ligand binding to yeast cells observed at temperatures needed to denature native Ste2p. We also explored the use of an alternative approach for assaying receptor stability based on loss of signaling function at elevated temperatures, monitored via transcriptional induction of a pheromone-responsive *FUS1*-lacZ reporter gene.[71] While loss of signaling was observed over the range of 30−40 °C, most of this loss, apparently, does not result from destabilization of receptors because ligand binding by wild-type Ste2p is unaffected by these treatments and because a similar temperature dependence of signaling is observed in strains in which the pheromone response pathway is activated in a ligand-independent fashion by deletion of *GPA1* encoding the G protein α-subunit (results not shown). Thus, the screen for stabilizing mutations was conducted by first isolating temperature-sensitive mutations conferring loss of receptor binding and signaling function at 34 °C and then isolating intragenic second-site suppressors that restore high levels of ligand binding to the temperature-sensitive alleles.

Isolation of Temperature-Sensitive Mutants of *STE2* Based on Loss of Signaling Function. To isolate temperature-sensitive alleles of *STE2*, we used error-prone PCR to randomly mutagenize a region of the full-length receptor that included the sequences encoding all seven predicted transmembrane segments and then screened yeast transformants for alleles conferring temperature-sensitive signaling based on resistance to α-factor-dependent growth arrest at 34 °C but not at 24 °C. From a library containing approximately 10000 clones, we isolated six temperature-sensitive alleles containing single-amino acid substitutions and seven additional alleles containing multiple-amino acid substitutions (Figure S3 of the Supporting Information and Table 1; a list of the phenotypes of individual mutations discussed herein is presented in Table S7 of the Supporting Information).

To determine whether the missense mutations in the *STE2* gene that were recovered in this screen were responsible for the observed phenotypes, the single mutations that elicited growth arrest phenotypes were reconstructed by recloning the

Table 1. Temperature-Sensitive Alleles Identified from the Growth Arrest and Binding-Based Screens

mutation	screen
S95Y	growth arrest
Q135H/L164P/S207I	growth arrest
I260K	growth arrest
G31R/M69K/S213F	growth arrest
H94Y	growth arrest
I53V/L113R	growth arrest
S104Y	growth arrest
V45A/V152L/T179I/Q253K	growth arrest
G31R/A52T	growth arrest
V49D	growth arrest
F55L/F116S/N158D	growth arrest
Q51P/G174W/G237S	growth arrest
L211R	growth arrest
F38Y	binding

DOI: 10.1021/bi501314t
Biochemistry 2015, 54, 1787−1806

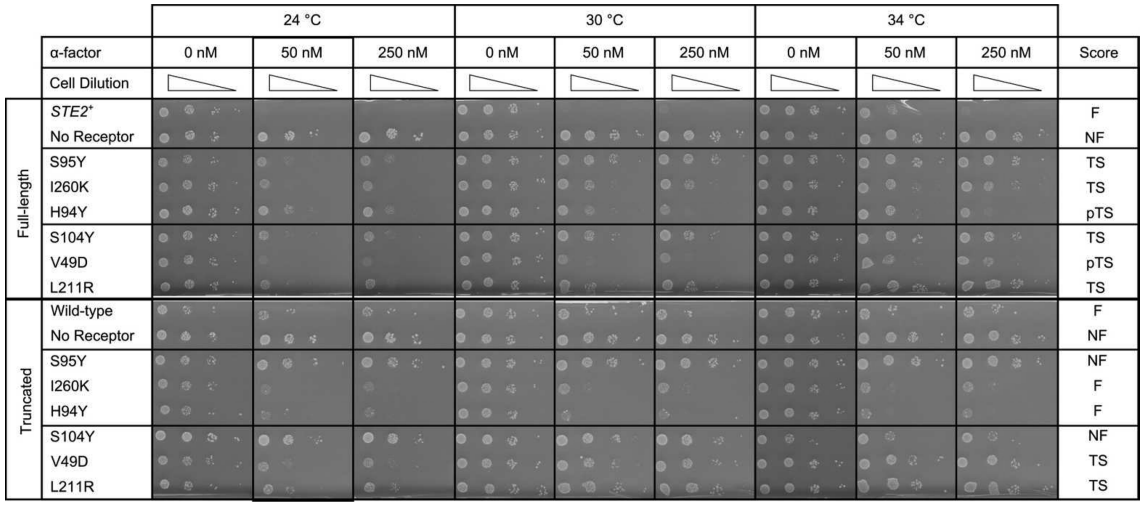

Figure 1. Temperature-sensitive receptors with single-amino acid substitutions exhibit a temperature-dependent growth phenotype. The figure shows the α-factor-dependent growth inhibition of clones that were reconstructed by transforming plasmids bearing missense mutations in either full-length *STE2* or C-terminally truncated *STE2* into the yeast host strain. Each panel shows the growth of four 10-fold serial dilutions of the relevant yeast strain in the presence of the indicated α-factor concentration. The clones were scored as functional (F), nonfunctional (NF), temperature-sensitive (TS), or partially temperature-sensitive (pTS).

sequenced regions of the mutated *STE2* genes into fresh plasmids and transforming a fresh yeast host. The growth arrest assay performed on these reconstructed strains, shown in Figure 1, verified that cells expressing receptors containing each of the six tested single-amino acid substitutions exhibit a temperature-sensitive growth phenotype in the presence of α-factor. (In this assay, growth of cells on medium containing α-factor indicates loss of signaling function such that growth at high temperatures but not low temperatures is characteristic of temperature-sensitivity of Ste2p.) Some of the single mutations also result in partial defects in growth arrest at 24 °C.

The only previously identified temperature-sensitive mutation in *STE2* is the A52T substitution, which was reported to result in a temperature-dependent loss of responsiveness to α-factor.[64,76] This substitution was recovered as part of a multiply substituted *STE2* allele exhibiting temperature-sensitive α-factor-dependent growth arrest. However, neither A52T nor the other mutation recovered in this allele, G31R, results in any detectable defect in growth arrest when tested individually by plating dilutions of culture on plates containing α-factor. This discrepancy may reflect that fact that the previous study of A52T[76] assayed growth arrest based on the sizes of inhibitory halos surrounding α-factor aliquots applied to culture plates, in contrast to the dilution assay reported here. The A52T substitution, when present as the only mutation in Ste2p, did result in decreased numbers of cell-surface-binding sites compared to wild-type receptors (with a greater decrease at 34 °C than at 24 °C) (Figure S4 of the Supporting Information).

In addition to the missense mutations conferring temperature sensitivity, we also recovered nine *STE2* alleles that displayed temperature-sensitive signaling apparently resulting from the presence of premature stop codons at various positions in the coding sequence for the receptor. Temperature-sensitive growth of these clones can be explained by the fact that the host strain used for these studies contains the temperature-sensitive termination suppressor *SUP4-3*^{ts}, which allows read-through of amber stop codons (UAG) at the low, permissive temperature.[77] This class of mutations was not studied further.

Mutated Receptors Exhibiting Temperature-Dependent Loss of Signaling Function Are Present at Reduced Abundances in Cells. Saturation binding experiments using the fluorescent α-factor analogue [K^7(NBD),Nle^{12}]-α-factor were used to compare the relative numbers of binding sites present on the external surface of cells expressing full-length normal and mutant receptors (Figure 2 and Table 2). When cultured at high temperature (34 °C), cells expressing most of the identified temperature-sensitive receptor variants exhibited very low levels of ligand binding that precluded measurement of the abundances and binding affinities of their receptors (Figure 2B,C and Table 2). Among the mutant full-length receptors isolated from the screen for loss of function, only the variant containing the V49D substitution retained a measurable number of cell-surface-binding sites at 34 °C. It was present at 40% of the level of similarly expressed full-length wild-type Ste2p and exhibited a 2-fold reduction in binding affinity for [K^7(NBD),Nle^{12}]-α-factor compared with wild-type full-length receptors at this temperature.

Reductions in levels of cell-surface binding were also observed in cells expressing mutant receptors cultured at the permissive temperature of 24 °C (Figure 2A and Table 2). Cells expressing the full-length H94Y and S104Y variants retained only ~30% of the wild-type number of sites, and greater reductions in numbers of sites were detected for most of the other temperature-sensitive variants. Only full-length receptors containing the V49D substitution were expressed at nearly wild-type levels at 24 °C. Affinities of the mutated receptors for the fluorescent ligand were similar to, or higher than, the affinity of the normal full-length receptor assayed at this temperature.

The screen used to identify these temperature-sensitive mutants is based on loss of signaling function at high temperatures, which could occur either through a temperature-sensitive defect in the signaling capacity of preexisting receptors or through a temperature-dependent reduction in the number of receptors at the cell surface. However, responses to

DOI: 10.1021/bi501314t
Biochemistry 2015, 54, 1787−1806

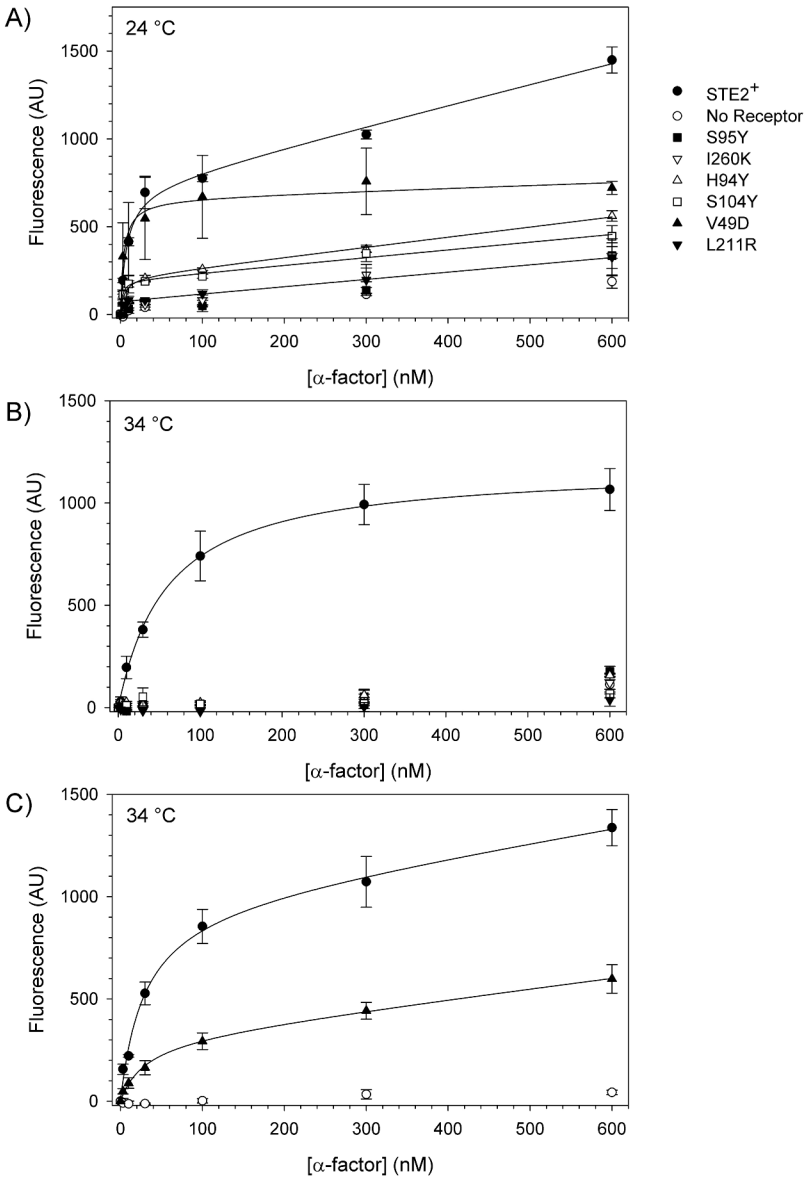

Figure 2. Full-length temperature-sensitive receptors isolated on the basis of loss of signaling function exhibit reduced numbers of binding sites at the cell surface. Strains expressing the indicated full-length *STE2* alleles were grown in liquid cultures at (A) 24 or (B and C) 34 °C. The error bars represent the standard error based on an assay of binding to three independent isolates of each strain. Binding was assessed by flow cytometry as described in Materials and Methods (parameters derived from fitting are listed in Table 2).

pheromone in yeast are not dependent on the abundance of Ste2p, as long as the number of receptors expressed at the cell surface exceeds a minimal threshold. Similar signaling responses are obtained for cells expressing *STE2* from a multicopy plasmid (at more than 10 times the level from the normal chromosomal *STE2* allele) and cells expressing *STE2* from a galactose-inducible promoter under repressing conditions (<20% of the normal level for chromosomal *STE2*).[68,78−80] Thus, for a mutation to result in a loss of signaling function that is purely caused by a reduction in the number of receptors at the cell surface, the mutation would have to severely reduce the level of cell-surface expression to below the threshold level. In fact, we observe only a weak correlation between the numbers of receptor variants present at the cell surface and retention of signaling function (Figure 1 and Table 2). The strongest signaling response among the full-length variants at 34 °C was observed for the receptor containing the H94Y substitution, which is present at the cell surface at low abundance. At the same time, the V49D variant, which is present at the highest abundance among tested full-length variants at 34 °C, exhibits a severe defect in α-factor-dependent growth arrest (Figure 1). The correlation between signaling and expression was also weak for cells cultured at 24 °C, where cells expressing the most abundant variant containing the V49D substitution exhibited robust pheromone-dependent growth arrest, but cells expressing the second most abundant variant (H94Y) exhibited weaker responses to α-factor than some of the variants with a much lower level of expression at the cell surface, such as those containing the L211R and I260K substitutions.

Effects of C-Terminal Truncation of Temperature-Sensitive Receptors. The C-terminal tail of Ste2p contains multiple sites implicated in endocytosis of receptors and downregulation of signaling. Thus, truncation of this tail results

DOI: 10.1021/bi501314t
Biochemistry 2015, 54, 1787−1806

Table 2. Ligand Binding Parameters of Temperature-Sensitive Receptors

	full-length receptors				C-terminally truncated receptors			
	34 °C		24 °C		34 °C		24 °C	
variant	relative B_{max} (% of wild-type value)	K_D (nM)	relative B_{max} (% of wild-type value)	K_D (nM)	relative B_{max} [a] (% of wild-type value)	K_D (nM)	relative B_{max} (% of wild-type value)	K_D (nM)
wild-type	100 ± 24	28 ± 4.7	100 ± 14	7.3 ± 0.9	1250 ± 240	45 ± 1.7	1250 ± 370	19 ± 3.8
F38Y	–[b]	–[b]	–[b]	–[b]	330 ± 62	64 ± 7.9	1100 ± 120	59 ± 11
V49D	37 ± 8	49 ± 20	80 ± 29	5.3 ± 2.3	100 ± 20	35 ± 4.0	290 ± 150	23 ± 3.3
H94Y	ND[c]	ND[c]	30 ± 4.2	5.2 ± 2.1	280 ± 53	90 ± 12	360 ± 100	47 ± 8.1
S95Y	ND[c]	ND[c]	3.2 ± 1.6	2.1 ± 1.5	ND[c]	ND[c]	7.0 ± 3.2	8.1 ± 7.5
S104Y	ND[c]	ND[c]	26 ± 3.0	2.0 ± 0.7	ND[c]	ND[c]	66 ± 22	12 ± 3.4
L211R	ND[c]	ND[c]	10 ± 2.1	0.8 ± 0.1	ND[c]	ND[c]	ND[c]	ND[c]
I260K	ND[c]	ND[c]	ND[c]	ND[c]	ND[c]	ND[c]	ND[c]	ND[c]

[a]Levels are relative to full-length wild-type receptor levels using a conversion factor of 12.5 ± 2.3, determined from the ratio of B_{max} values that were fit to strains expressing either full-length or truncated wild-type receptors (Figure S2 of the Supporting Information). The conversion factor was measured at only 24 °C and applied to both temperatures. [b]Not tested. [c]Not detectable.

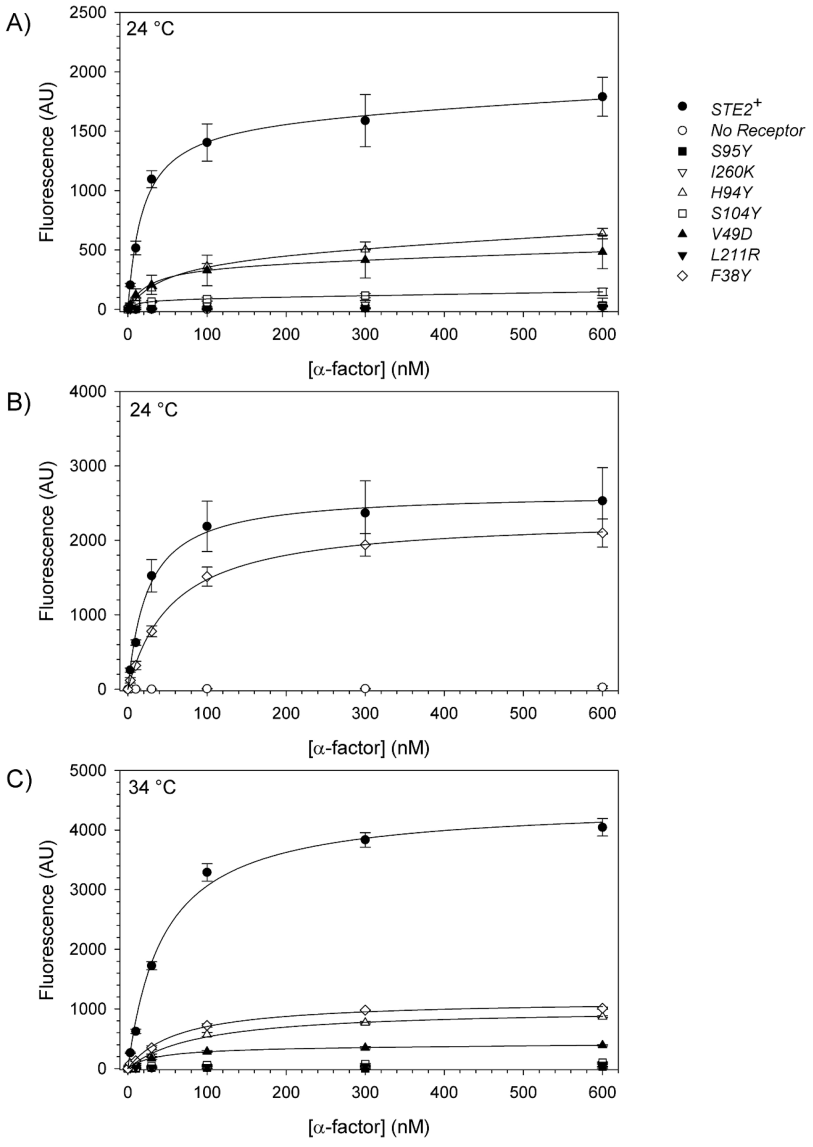

Figure 3. C-Terminally truncated temperature-sensitive receptors express reduced numbers of binding sites at the cell surface. Strains expressing the indicated truncated *STE2* alleles were grown in liquid cultures at (A and B) 24 or (C) 34 °C. The error bars represent the standard error based on an assay of binding to three independent isolates of each strain. Binding was determined by flow cytometry as described in Materials and Methods (parameters derived from fitting are listed in Table 2).

DOI: 10.1021/bi501314t
Biochemistry 2015, 54, 1787–1806

in increased levels of receptor cell-surface expression and hypersensitive signaling responses.[78,79] While our initial screen for temperature-sensitive signaling function was conducted using full-length *STE2* alleles, the identified temperature-sensitive single-amino acid substitutions were subsequently transferred into receptors that were C-terminally truncated at K304 to facilitate assays of ligand binding (see Figure 3 and Table 2). C-terminally truncated receptors that were otherwise wild-type were expressed at the cell surface at levels approximately 10 times higher than those of full-length wild-type receptors (Figure S5 of the Supporting Information). At 34 °C, cell-surface levels of two variants (V49D and H94Y) were considerably higher than the levels observed for full-length receptors with the same substitutions. At 24 °C, the cell-surface abundances of the V49D and H94Y truncated variants were approximately 4 and 12 times higher, respectively, than the levels of the full-length form with the same mutation. However, the abundances of some mutants (S95Y and S104Y) increased to lesser extents upon truncation. Binding to the truncated form of the L211R variant could not be detected at either 24 or 34 °C, despite the fact that binding to the full-length variant was detected at 24 °C, indicating that C-terminal truncation of this allele actually results in a decrease in cell-surface abundance. The affinities of the truncated forms of Ste2p for ligand were generally somewhat lower than the affinities of full-length forms with the same substitutions (but differed from that of the truncated wild type by a factor of less than 3).

In cases in which a decreased level of binding of ligand to variant forms of Ste2p is seen at elevated temperatures, the decrease in the level of binding could result either from a decreased rate of delivery of newly synthesized receptors to the plasma membrane during cell growth at high temperatures or from temperature-induced unfolding or degradation of receptors that are already present at the cell surface. However, when cells expressing C-terminally truncated Ste2p variants that were initially cultured at 24 °C were treated for 30 min at increasing temperatures (up to 52 °C), no progressive loss of binding sites was observed (Figure S6 of the Supporting Information). This indicates that the observed reductions in the numbers of sites are due to a reduced level of synthesis or trafficking rather than unfolding or degradation of preexisting receptors.

Isolation of Temperature-Sensitive Alleles of *STE2* Based on Temperature-Sensitive Loss of Ligand Binding. To directly identify temperature-sensitive mutations resulting in loss of binding sites at high temperatures while maintaining high abundances of sites at low temperatures, we conducted a second screen of randomly mutated *STE2* alleles based only on ligand binding considerations. This screen was conducted in two stages. The first stage used fluorescence-activated cell sorting (FACS) to identify clones that express high numbers of receptors competent for ligand binding at the cell surface at 24 °C, confirming that the selected population is capable of folding to form a native ligand-binding site at the low temperature. The second stage used FACS to sort for clones with reduced numbers of ligand-binding sites at 34 °C. This screen was conducted using cells expressing C-terminally truncated receptors to enhance the strength of the signal from bound fluorescent ligand binding (see Figure S5 of the Supporting Information).

From a library of ~115000 strains expressing randomly mutagenized truncated receptor, we identified three different alleles with the desired phenotype. (1) One of the alleles encoded a single-amino acid substitution, F38Y, in the N-terminal extracellular portion of Ste2p. (2) A second allele contained two substitutions, N46I and V49D. The V49D substitution had already been identified as resulting in temperature sensitivity of signaling function (Figures 1 and 2). (3) The third allele included three substitutions, one of which was N158Y at the same position as a mutation that had been classified as having a medium effect on ligand binding (N158D), whose effects had not been tested in truncated receptors. The temperature-sensitive ligand-binding phenotypes of these three alleles were confirmed following retransformation into fresh yeast hosts (Figure 4). All three

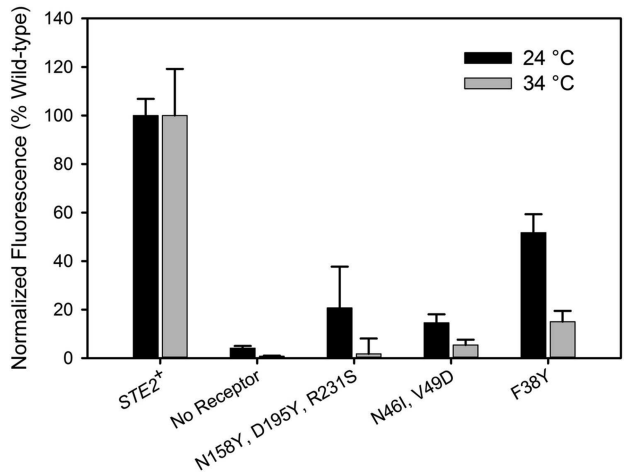

Figure 4. Temperature dependence of binding of ligand to cells expressing temperature-sensitive receptors isolated on the basis of the loss of ligand binding. The graph shows the fluorescence of bound [K^7(NBD),Nle^{12}]-α-factor determined by flow cytometry following growth at 24 and 34 °C and incubation with 300 nM [K^7(NBD),Nle^{12}]-α-factor. The assay was performed using cells that had been retransformed with plasmids isolated from clones derived from the original screen. The error bars represent the standard error based on an assay of binding to three independent isolates of each strain.

variants exhibit fewer binding sites at 34 °C than at 24 °C. Furthermore, consistent with the goal of screening for mutations with less severe ligand-binding phenotypes that may not be sufficient to interfere with signaling responses, the F38Y substitution exhibits no detectable loss of growth arrest (results not shown).

Additivity of Effects of Destabilizing Mutations Identified in Temperature-Sensitive Mutants Containing Multiple Amino Acid Substitutions. To determine the phenotypes of individual mutations recovered in the seven multiply substituted alleles recovered in the screen for temperature-sensitive loss of signaling function, all of the individual substitutions recovered in these alleles were re-created by site-directed mutagenesis and tested individually for their effects on growth arrest and ligand binding of full-length receptors. Surprisingly, although they exhibited various effects on ligand binding, only one of the 17 tested mutations, L113R, exhibited a growth phenotype that differed from the wild-type phenotype when introduced individually into Ste2p (Figure S7 of the Supporting Information). Thus, the observed signaling defects of the remainder of the multiply substituted alleles must result from additive effects of multiple mutations acting together.

DOI: 10.1021/bi501314t
Biochemistry 2015, 54, 1787−1806

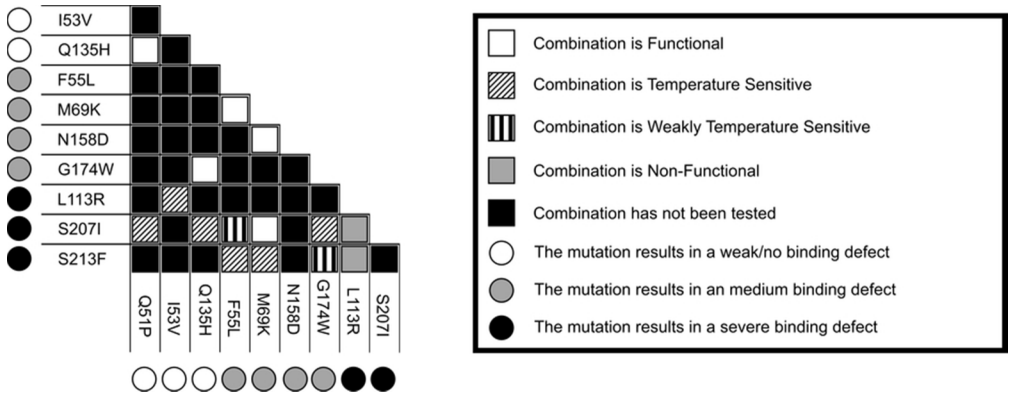

Figure 5. Pattern of additivity of individual temperature-sensitive mutations that did not yield temperature-sensitive growth arrest as single substitutions. On the axes, the color of the circles indicates the effect of the mutation alone on the number of cell-surface ligand-binding sites. The fill pattern of the squares at the intersection of two mutations indicates the effect of the combination of the two mutations, as measured by a growth arrest assay.

Additivity of mutational effects could arise through specific interactions among mutated residues, or it could be the result of incremental effects on global protein stability, where the effects of each individual mutation are too small to elicit a growth phenotype. To distinguish between these possibilities, we tested the effects of combining individual mutations derived from different multiply substituted temperature-sensitive alleles into new doubly substituted alleles. In deciding which mutations to incorporate into these new alleles, we categorized each characterized individual mutation as "severe", "medium", or "weak", based on its effect on ligand binding (Figure S8 of the Supporting Information). Mutations classified as "weak" resulted in high levels of cell-surface receptors that were statistically indistinguishable from levels of wild-type Ste2p. Mutations classified as "severe" resulted in levels of ligand binding that were reduced to less than ~30% of wild-type levels. The category of mutations classified as "medium" included all alleles that resulted in numbers of binding sites that were intermediate between those of the severe and weak categories. A sampling of the possible combinations of each type of pairing (severe−severe, severe−medium, severe−weak, etc.) was constructed by site-directed mutagenesis, transformed into yeast, and assayed for temperature-dependent growth arrest (Figure S9 of the Supporting Information and Figure 5). The results can be summarized as follows. (1) Combination of two individual weak mutations, a weak with a medium mutation, or two medium mutations all resulted in receptor variants with α-factor-dependent growth arrest indistinguishable from that conferred by wild-type Ste2p. (2) Combinations of two individual severe mutations resulted in receptors that exhibited no detectable function at any temperature in the growth arrest assay. (3) Combinations of medium mutations with severe mutations always yielded receptors with at least partial function, ranging from fully functional at all temperatures (S207I/M69K) to strongly temperature-sensitive (S213F/F55L and S213F/M69K).

A possible explanation of the additive effects of the mutations recovered from multiply substituted alleles could be that the individual substitutions cause modest changes in the levels of receptors at the cell surface such that the population of receptors remains higher than the threshold required for a full signaling response,[68,78−80] whereas combinations of substitutions that exhibit measurable phenotypes reduce the numbers of receptors below this threshold. As a test of this idea, we examined the effects of reducing the level of expression of the receptors containing individual mutations by encoding the mutant genes on centromere-based *CEN* plasmids, expected to provide a 5−10-fold reduction in the level of cell-surface expression compared to that of the multicopy plasmids used elsewhere in this study.[74] When 21 strains with *CEN* plasmids expressing individual mutations derived from multiply substituted STE2 were assayed for growth arrest in the presence of α-factor at different temperatures (Figure S10 of the Supporting Information), most showed phenotypes indistinguishable from what was observed with multicopy plasmids. However, three variants (containing the L113R, Q135H, and S207I substitutions) that exhibited no signaling phenotypes when expressed from multicopy plasmids did, in fact, exhibit diminished growth arrest at high temperatures when expressed from *CEN* plasmids. The variant containing the S207I substitution is expressed at relatively low levels when encoded on a multicopy plasmid (Figure S8 of the Supporting Information); thus, reduction of the gene copy number may further reduce the number of cell-surface receptors below a threshold required for signaling. However, this explanation does not apply to the observed signaling defect of the Q135H variant, because this Ste2p containing the Q135H substitution is present at the cell surface at nearly wild-type levels when encoded on a multicopy plasmid. Thus, the basis for the signaling defect of the *CEN* plasmid-encoded Q135H variant remains unclear.

Identification of Suppressors of Temperature-Sensitive Mutations. To identify mutations likely to enhance the thermal stability of the yeast α-factor receptor Ste2p, we conducted random mutagenesis of temperature-sensitive *STE2* alleles and screened for second-site intragenic suppressors of temperature-sensitivity using FACS to identify clones that maintain high numbers of cell-surface-binding sites for [K^7(NBD),Nle^{12}]-α-factor following treatment at elevated temperatures. Libraries of mutagenized C-terminally truncated *STE2* genes were constructed by error-prone PCR of templates encoding four different temperature-sensitive alleles (V49D, S95Y, S104Y, and I260K). Each of the four libraries contained approximately 100000 clones. A gate for sorting was established using a two-dimensional analysis in which the fluorescence of bound ligand is plotted against the forward scattering, an indication of cell size (Figure S2 of the Supporting Information). The gate was set to collect the 1% of cells

DOI: 10.1021/bi501314t
Biochemistry 2015, 54, 1787−1806

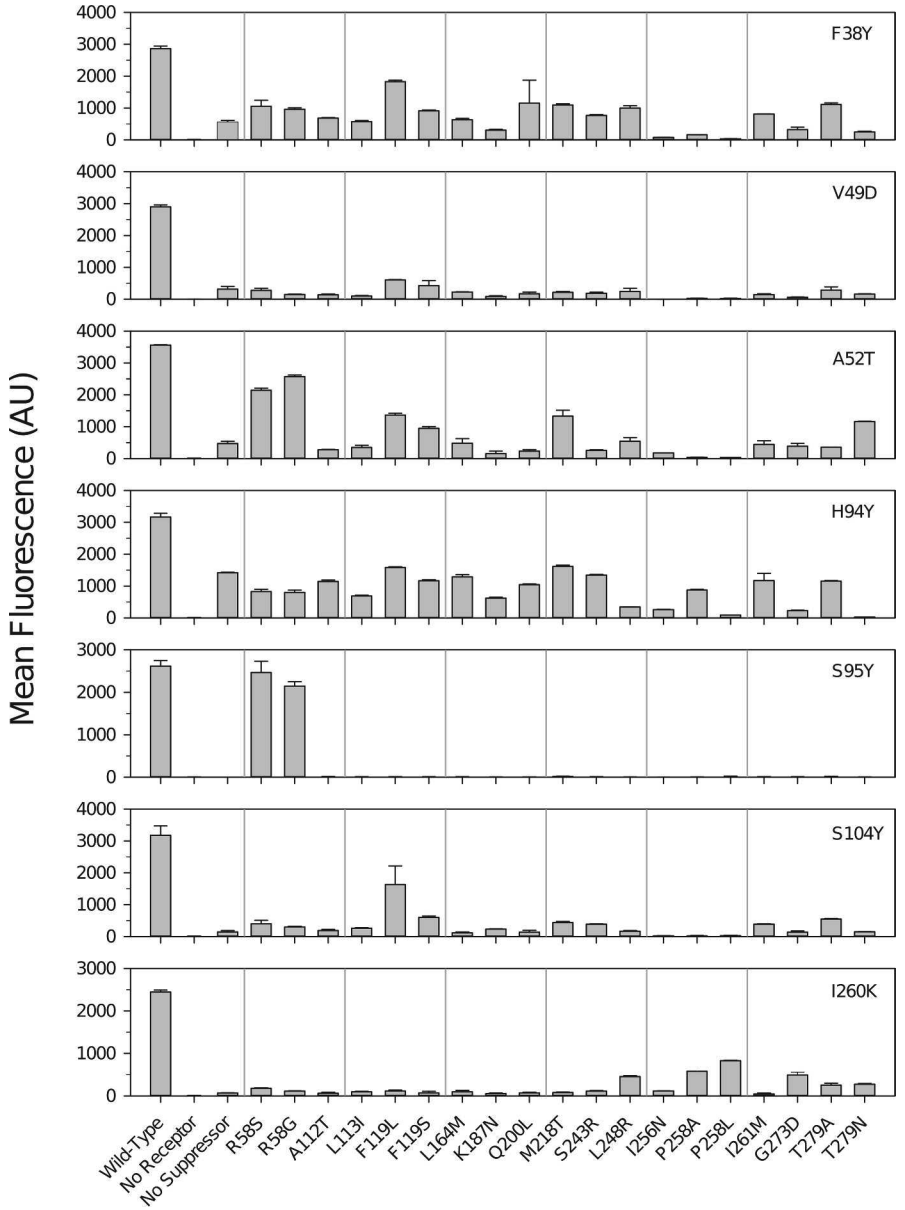

Figure 6. Ligand binding assays performed on yeast strains in the double-mutant array. Strains were cultured overnight at 30 °C (34 °C for F38Y and A52T mutants) and assayed for ligand binding with 300 nM fluorescent α-factor. The error bars represent the standard error based on an assay of binding to three independent isolates of each strain.

exhibiting the highest levels of bound fluorescent ligand (of 200000 sorted cells).

A total of 72 clones collected from each library were recultured and assayed for fluorescent ligand binding levels at a saturating ligand concentration. Of the 288 clones tested, 101 exhibited increased levels of ligand binding compared to the levels of fluorescence for the relevant starting allele. {When 10 randomly selected plasmids encoding examples of these alleles were transferred to a fresh yeast host and tested for binding of [K^7(NBD),Nle^{12}]-α-factor, nine of them resulted in increased numbers of cell-surface ligand-binding sites compared with the control temperature-sensitive allele (data not shown), indicating low levels of false positives in this pool of suppressed alleles.} The sequence changes observed in the *STE2* genes from all the confirmed clones isolated in the suppressor screen (omitting duplicate clones, clones with reversions, and clones containing only silent mutations) are listed in Table S8 of the Supporting Information. Mutations that were recovered from multiple mutagenized libraries, mutations that were recovered from multiple independent clones within a single library, and mutations that were recovered from alleles containing only a single-amino acid substitution (other than the temperature-sensitive starting mutation) were selected for further analysis. The allele with the highest level of suppression (R58G/S95Y) restored ~65% of the wild-type number of receptors; most of the suppressed alleles restored levels to less than 35% of wild-type levels. Several of the recovered second-site mutations also suppressed temperature-sensitive defects in pheromone-dependent cell cycle arrest (Figure S11 of the Supporting Information).

Testing for Global Suppression in an Array of Site-Directed Double Mutants. To determine the extent to which the identified suppressor mutations can suppress different temperature-sensitive mutations, site-directed mutagenesis was

DOI: 10.1021/bi501314t
Biochemistry 2015, 54, 1787−1806

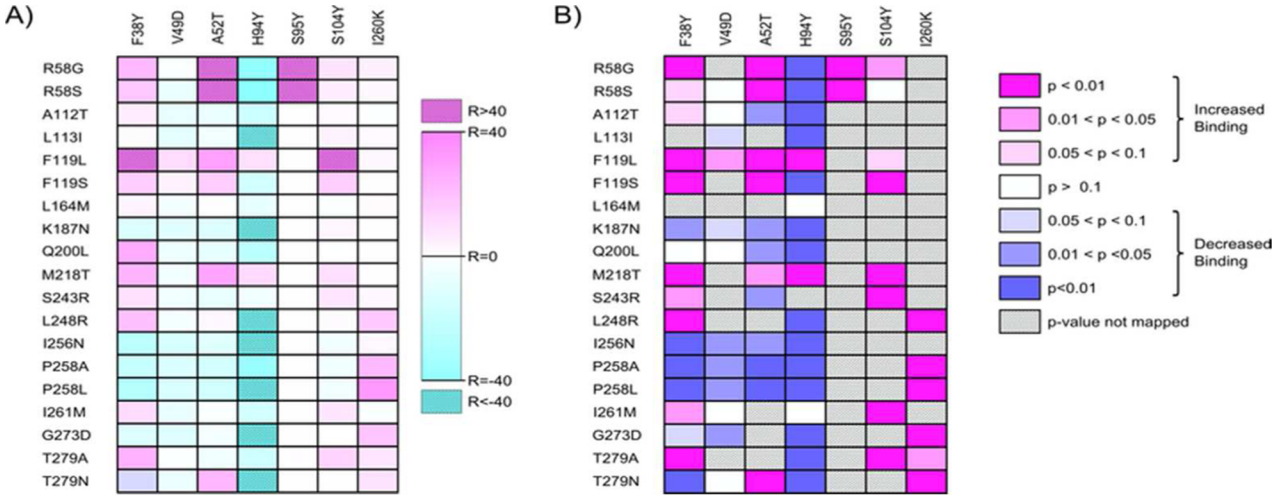

Figure 7. Summary of the effects of combinations of suppressor and temperature-sensitive mutations on numbers of ligand-binding sites at the cell surface. The temperature-sensitive mutations are listed across the top of the tables. Suppressor mutations are listed along the sides. (A) Each mutation pair was scored using the metric *R*, defined as the difference between the fluorescence of the double mutant and the temperature-sensitive single mutant divided by the difference between the wild type and the temperature-sensitive single mutant, as a measure of the recovery of ligand binding levels due to the suppressor. Magenta boxes indicate a positive effect of the suppressor mutation on ligand binding levels, while cyan boxes indicate that the suppressor mutation had a negative effect on ligand binding levels. Note that the scale is clipped to better highlight the intermediate effects. (B) The indicated *p* values refer to the comparison of the ligand binding of the double mutant to that of the temperature-sensitive mutant alone. Only *p* values for double mutants with an *R* value of more than 5 or less than −5 were mapped. Magenta boxes indicate the significance of the *p* values for alleles showing enhanced ligand binding resulting from suppression. Blue boxes indicate the significance of the *p* values for alleles showing a decreased level of ligand binding resulting from a combination of the two mutations.

used to create a double-mutant array consisting of all possible combinations of seven different temperature-sensitive mutations with 19 different suppressor mutations isolated from the mutagenic libraries. To provide additional breadth for the testing of the "global" nature of the suppressors, the temperature-sensitive mutations F38Y, A52T, and H94Y were included in the double-mutant array even though these mutations had not served as templates for any of the libraries that were screened for suppressors. Cells expressing each component of the double-mutant array were assayed for ligand binding under saturating conditions after growth at restrictive temperatures (Figure 6) and for the ability to elicit growth arrest in response to α-factor, assayed at permissive and restrictive temperatures, by serial dilution onto solid medium containing different concentrations of α-factor (Figures S12–S15 of the Supporting Information). The tested restrictive temperature for the double mutations including the F38Y or A52T substitution was 34 °C, the temperature at which a temperature-dependent loss of ligand binding is observed.[64] The tested restrictive temperature for the double mutations including substitution V49D, H94Y, S95Y, S104Y, or I260K was 30 °C, the minimal temperature at which a temperature-dependent loss of growth arrest is observed. The quantitation of percent recovery, calculated as "*R* values", is displayed as a heat map in Figure 7A, and the statistical significance of the observed suppression for each combination is displayed as a second heat map in Figure 7B.

Of the 19 original suppressor mutations, 14 exhibited significant suppression of the loss of cell-surface-binding sites for at least one temperature-sensitive starting allele (Figure 6). Seven of these suppressed more than one starting allele (Figure 7; $R > 10$, $p < 0.01$). The five R58S, R58G, F119L, F119S, and M218T mutations provided the most general global suppression, each enhancing ligand binding to at least three different temperature-sensitive mutations. In addition to their effects on receptor abundance, several suppressor mutations also at least partially reversed the temperature-sensitive signaling defects of starting alleles (Figures S12–S15 of the Supporting Information) as indicated by the reduced rate of growth of the double-mutant strain on α-factor-containing plates at 34 °C compared with that of cells expressing the starting allele alone (termed "temperature-sensitive" in Figures S12–S15 of the Supporting Information). By this criterion, the R58S substitution improved the signaling of the temperature-sensitive S95Y, I260K, and V49D Ste2p variants and the F119L and F119S substitutions both improve the signaling of the S95Y and S104Y variants. In accordance with previous results,[81] the R58G substitution retains full signaling function in a quantitative assay of transcriptional induction of the *FUS1*-lacZ reporter gene.[81] Similar confirmation of signaling function was obtained for R58S and F119L substitutions (results not shown). No signaling assays are shown for suppressors of temperature-sensitive starting mutations that do not exhibit defects in signaling at any temperature (H94Y and F38Y).

Interactions between Mutations of R58 and S95 Exhibit Partial Allele Specificity. Substitutions R58G and R58S provide suppression of multiple temperature-sensitive mutations, but their suppression of the S95Y starting mutation is particularly strong [restoring greater than 90% of wild-type levels of binding for the doubly substituted receptors compared to less than 1% for S95Y alone (see Figures 3 and 6)]. Furthermore, the two mutations at R58 were the only recovered substitutions that suppress the temperature-sensitive allele S95Y. This suggested that genetic interactions between positions 58 and 95 might include a specific component, reflecting direct interaction between amino acids at those two positions. On the basis of a homology model of Ste2p that was generated through comparison to the rhodopsin structure,[82] S95 and R58 are predicted to be in close proximity (Figure S16 of the Supporting Information). A simple explanation of the

DOI: 10.1021/bi501314t
Biochemistry 2015, 54, 1787–1806

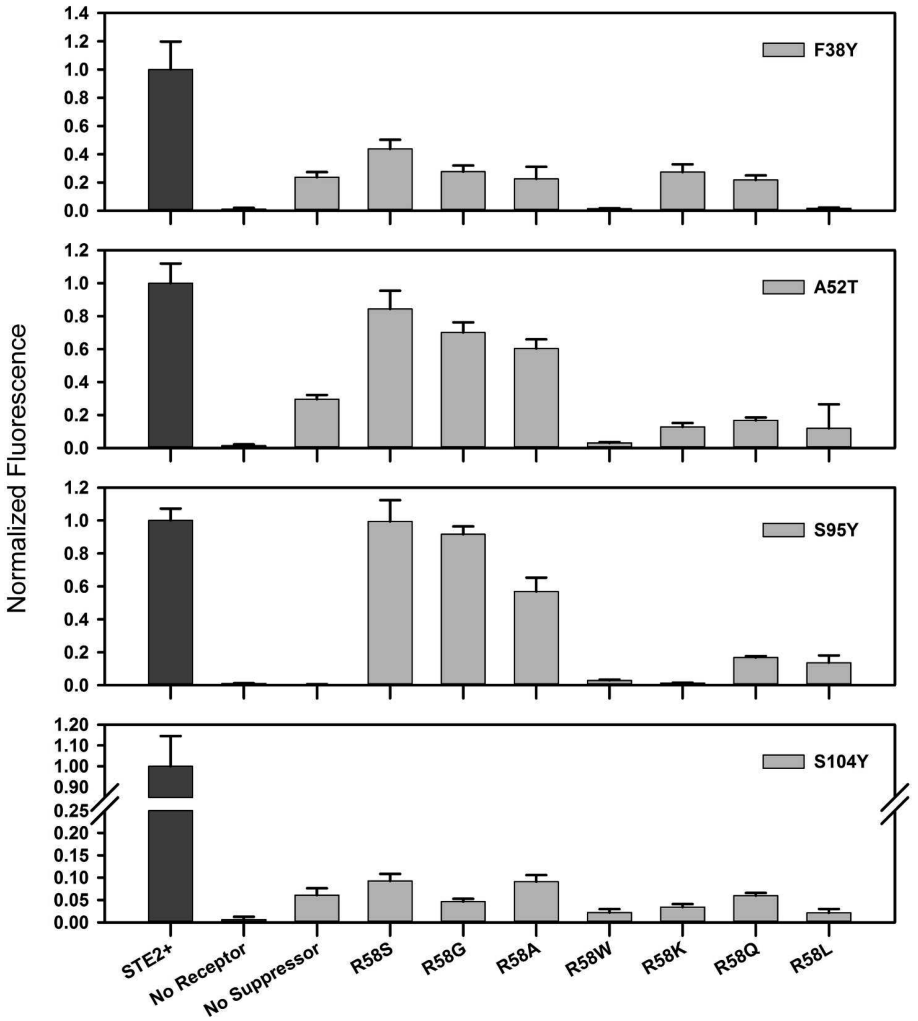

Figure 8. Suppression of different temperature-sensitive mutations by site-direct substitutions at position R58. Binding of [K^7(NBD),Nle^{12}]-α-factor to cells was conducted as described in Materials and Methods at a ligand concentration of 300 nM. For the clones containing the S95Y and S104Y mutations, ligand binding was measured after growth at 30 °C. For the clones containing the A52T and F38Y mutations, ligand binding was measured after growth at 34 °C. The error bars represent the standard error based on an assay of binding to three independent isolates of each strain.

observed interaction is that replacing R58 with a residue with a smaller side chain (R58G and R58S) relieves steric clash resulting from replacing S95 with a residue with a larger side chain (S95Y). To test this hypothesis, seven different R58 substitutions (R58A, R58G, R58L, R58K, R58Q, R58S, and R58W) involving replacement of R58 with side chains of different sizes, polarities, and charges were assayed for their effects on ligand binding at restrictive temperatures (either 30 or 34 °C) when combined with four different temperature-sensitive starting mutations (F38Y, A52T, S95Y, and S104Y). Consistent with the idea that suppression arises, at least in part, from relief of steric clash, introduction of alanine at position 58 also suppressed the temperature-sensitive loss of binding sites resulting from the S95Y mutation, increasing the number of cell-surface-binding sites to ~55% of wild-type levels (Figure 8). However, the presence of alanine at position 58 (a substitution that has previously been reported to reduce the level of ligand binding[83,84]) also provides an element of global suppression, because this substitution also partially suppresses the temperature-sensitive mutations A52T and S104Y. Substitution of tryptophan or lysine for R58 provided only very weak (2.8 or 1.2% of the wild-type level, respectively) suppression of S95Y, while substitution of glutamine or leucine provided intermediate (16.8 or 13.7% of the wild-type level, respectively) levels of suppression. None of these substitutions of larger residues for R58 provided any suppression of the temperature-sensitive mutations other than S95Y.

Effects of Some Combinations of Suppressors Are Additive. As a test of whether the effects of the identified suppressor mutations are additive, *STE2* alleles encoding various combinations of global suppressors R58S, F119L, and M218T with temperature-sensitive mutations A52T and F38Y were created by site-directed mutagenesis. Strains expressing these alleles were assayed for fluorescent ligand binding under saturating conditions after overnight growth at 34 °C (Figure 9). For one of the temperature-sensitive starting alleles (A52T), all combinations of suppressor mutations exhibit stronger effects than individual mutations in restoring ligand binding (Figure 9). The particular combination of R58S and F119L restores the full level of wild-type ligand binding. For another starting allele, F38Y, one suppressor, F119L, provides restoration of ligand binding for cells cultured at high temperatures (to ~70% of the wild-type abundance), but no combination of F119L with additional suppressors provided any improvement over F119L alone. However, the combination of weaker suppressors R58S and M218T together with F38Y

DOI: 10.1021/bi501314t
Biochemistry 2015, 54, 1787−1806

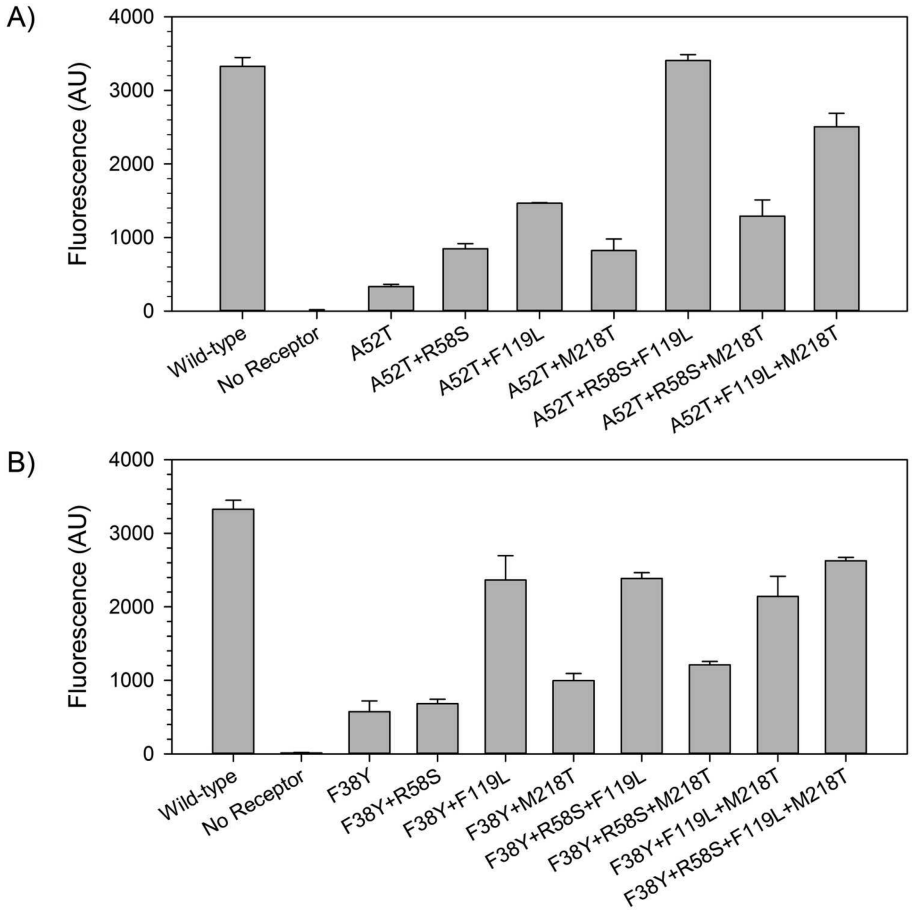

Figure 9. Global suppressors identified from the double-mutant array exhibit additive effects on ligand binding. Combinations of global suppressor mutations R58S, F119L, and M218T with temperature-sensitive mutations (A) A52T and (B) F38Y were constructed by site-directed mutagenesis. Assays of binding of [K^7(NBD),Nle^{12}]-α-factor were performed using 300 nM ligand on cells cultured at 34 °C. The error bars represent the standard error based on an assay of binding to three independent isolates of each strain.

did result in slightly higher levels of ligand binding than either of these two suppressors alone.

Suppressor Mutations Stabilize the Receptor in the Absence of Temperature-Sensitive Starting Mutations. To determine whether the identified suppressor mutations provide stabilization of otherwise wild-type receptors that will facilitate purification and crystallization of Ste2p, it will be necessary to examine the stabilities of mutant receptors in a solubilized state useful for crystallization trials. However, our laboratory has, to date, been able to achieve only very poor yields of purified solubilized Ste2p receptors, despite relatively high expression levels in cells. Furthermore, while C-terminal truncation generally leads to increased levels of Ste2p expression at the cell surface, previous attempts to purify the C-terminally truncated forms of the receptor have been less successful than the application of similar procedures to full-length Ste2p (N. Fedoriw, K. Clark, and M. Dumont, unpublished results). In view of these difficulties, we have focused on the development of initial stages of a purification procedure involving immobilization of receptors on small (8 μm) polystyrene beads, so that purification of correctly folded receptors can ultimately be monitored by quantitation of binding of fluorescent ligand using flow cytometry. Immobilization via the triple c-myc epitope tag fused to the C-terminus of the truncated Ste2p is achieved through the use of mouse anti-myc antibodies in conjunction with beads that are coated with goat anti-mouse antibodies. Dodecyl maltoside was used as a detergent for solubilization, based on its effective solubilization of yeast proteins in general, and its use in previously reported purifications of Ste2p.[61−63,85]

In initial experiments, only very low yields of bead-bound receptors could be detected by immunoblotting of material eluted from the beads using SDS and urea. However, as shown in Figure 10, the presence of 300 nM α-factor during solubilization and immobilization dramatically improved the yield of Ste2p bound to beads for all the Ste2p variants tested. (Immunoblotting of Ste2p typically gives rise to multiple closely spaced bands, corresponding to differentially glycosylated and phosphorylated forms of the protein.[86]) Stabilization of solubilized Ste2p by ligand binding has been reported previously.[61] Because the conformational state of a protein would not necessarily be expected to affect accessibility of an appended epitope tag, the observed failure of Ste2p to bind to bead-conjugated anti-tag antibodies in the absence of ligand indicates that instability of solubilized Ste2p causes the protein to adopt a state that leads to aggregation or precipitation. This observed ligand dependence of bead binding demonstrates the existence of a population of solubilized receptors that retain the capability to bind ligand with high affinity, because the presence of a low concentration of ligand is sufficient to maintain Ste2p in a state that allows the attached epitope tag to bind immobilized antibody.

DOI: 10.1021/bi501314t
Biochemistry 2015, 54, 1787−1806

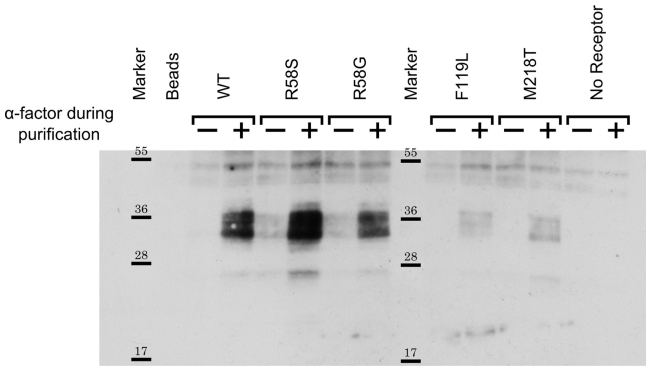

Figure 10. Effects of the presence of α-factor and suppressor mutations on the yield of immobilization of Ste2p. The indicated C-terminally truncated Ste2p variants were solubilized using dodecyl maltoside, in the presence or absence of 300 nM α-factor, and then incubated for 2 h at 24 °C with beads coated with anti-c-myc antibodies. To determine the amount bound, the Ste2p was then stripped from the beads using SDS/urea buffer and subjected to immunoblotting, probed with anti-c-myc antibodies.

We compared immobilization of receptors containing four different suppressor mutations (in the absence of temperature-sensitive mutations) with that of normal receptors in the presence and absence of α-factor (Figure 10). Solubilized forms of two variant receptors containing the suppressors R58G and R58S bind to antibody-coated beads in the presence of α-factor with approximately the same yield as wild-type receptors. However, in the absence of α-factor, receptors containing either of these substitutions bind to beads at levels that, while still low, are considerably greater than the yield of wild-type Ste2p. Even in the presence of α-factor, the binding yields of variants containing two other suppressor mutations, F119L and M218T, are lower than those for wild-type receptors, either because these variants are less stable or because they are produced in cells at levels lower than those of wild-type receptors. In either case, these results fail to provide evidence of stabilization of otherwise wild-type receptors by the F119L and M218T substitutions.

To examine the basis for the loss of Ste2p during purification, the fates of wild-type and R58G variant forms of the protein were monitored by immunoblotting of the samples based on the c-myc tag following incubation of solubilized receptors for different amounts of time in the presence of 0.1% DDM at room temperature (Figure S17 of the Supporting Information). While both the wild-type and mutant proteins migrated predominantly as monomers with a component of dimer, an additional population of higher-order oligomers was detected as a function of incubation time for the normal Ste2p receptors but not for the R58G variants.

DISCUSSION

Destabilizing Mutations of Ste2p Receptors. High levels of nonspecific binding and the inviability of yeast cells treated at high temperatures prevented the use of ligand binding as a basis for directly screening for mutations enhancing the thermostability of the Ste2p receptor. Thus,

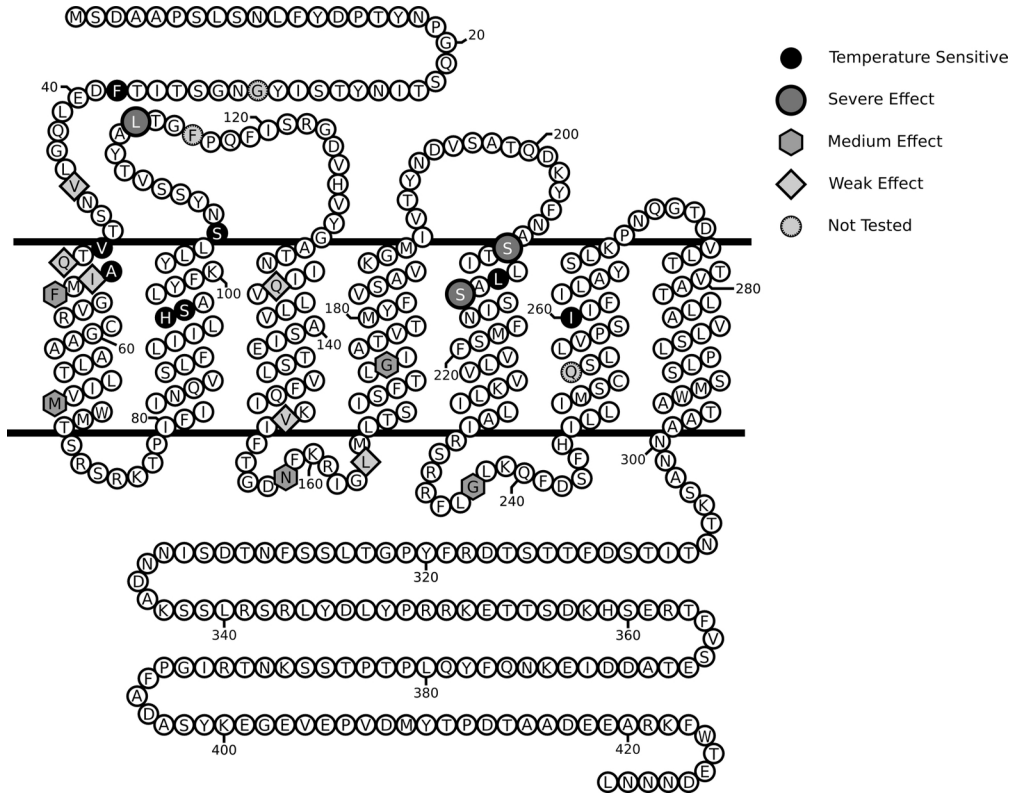

Figure 11. Distribution of temperature-sensitive mutations in Ste2p. The figure shows the predicted topology of Ste2p.[81] Residues in circles with a black background are sites at which single substitutions cause temperature-sensitive phenotypes. The other highlighted residues have been found to confer temperature sensitivity only when they are present in alleles with multiple-amino acid substitutions. The residues in enlarged circles had substitutions that caused large decreases in the level of ligand binding. The residues in hexagons had substitutions that caused moderate decreases in the level of ligand binding, while the residues in diamonds had substitutions that caused small decreases in the level of ligand binding.

DOI: 10.1021/bi501314t
Biochemistry 2015, 54, 1787−1806

we pursued an approach involving the isolation of temperature-sensitive mutations in the receptor that could be used as starting alleles for the isolation of stabilizing second-site intragenic suppressor mutations. Two screens, one for receptors with a reduced level of signaling function and the other for receptors present at reduced levels at the cell surface, yielded a total of seven temperature-sensitive alleles encoding single-amino acid substitutions. These substitutions are localized to the extracellular N-terminus of the receptor as well as to the extracellular side of predicted transmembrane helices 1, 2, 5, and 6 as shown in Figure 11. Their distribution on different helices and different predicted helical faces suggests that there is no single core of the receptor that provides structural stability but is generally consistent with the previously observed predominance of mutations affecting stability in extracellular regions of other GPCRs[51] and the apparent lower tolerance of the extracellular surface of GPCRs to mutation, compared with intracellular regions.[52] On the basis of the low frequencies at which these substitutions were recovered, it is likely that the alleles we recovered represent only a small fraction of the range of destabilizing mutations that are possible in the *STE2* gene.

Seven temperature-sensitive alleles containing multiple-amino acid substitutions were recovered from the screens that we conducted for mutations conferring temperature-sensitive α-factor-dependent growth arrest. We were surprised to find that, with one exception (L113R), the 17 individual mutations from these multiply substituted alleles did not, by themselves, exhibit any temperature-sensitive effects on receptor signaling, although some did result in decreased numbers of cell-surface-binding sites. Attempts to enhance the signaling phenotypes of these individual substitutions by decreasing plasmid copy number (from multicopy, at ~40 copies per cell, to *CEN*, at 1−3 copies per cell) were not generally successful. Thus, either the receptor expression level is not the limiting factor in signaling by the multiply substituted alleles, or cell-surface levels of receptors containing these individual mutations, even when expressed at low copy number, are above the threshold required for effective signaling; therefore, combinations of mutations are required to reduce the level of cell-surface expression below this threshold. The diversity of this type of multiply substituted temperature-sensitive alleles indicates that a large number of amino acid substitutions with no obvious phenotype as single mutations are capable of rendering Ste2p temperature-sensitive when present in combination with additional amino acid changes.

To test the specificities of interactions among mutations, we assayed the growth arrest phenotypes of 15 different reshuffled combinations of amino acid substitutions originally recovered in the multiply substituted alleles. Eight of the new combinations resulted in temperature-sensitive growth arrest phenotypes; two resulted in nonfunctional receptors at high and low temperatures, and five resulted in a functional receptor that was not temperature-sensitive. This indicates that the observed phenotypes of the combined mutations do not generally result from specific interactions between mutated sites but instead reflect additive or synergistic effects of incremental destabilization by the individual substitutions. Such additivity or synergy of effects on protein stabilization is consistent with the idea that stabilized proteins can be constructed by combining single mutations providing small individual enhancements in stability.[5,87]

All of the temperature-sensitive receptor variants that we isolated, including those identified on the basis of loss of signaling function, are present at the cell surface at reduced levels compared to the levels of equivalent (full-length or truncated) wild-type receptors. Furthermore, in all cases in which the levels at the cell surface were high enough to be measured, the numbers of cell-surface-binding sites on cells expressing the variant receptors were lower at 34 °C than at 24 °C. Some temperature-sensitive variant receptors were present at such low levels on cells at 24 °C that it is likely that a further reduction in the numbers resulting from growth at 34 °C was sufficient to reduce receptor abundance below a threshold required in the yeast system for effective signaling. However, reduced receptor abundance does not provide an explanation for all the observed effects of the identified temperature-sensitive mutations. For example, C-terminally truncated forms of receptors containing amino acid substitutions V49D and H94Y exhibit defects in signaling at 34 °C (Figure 1) even when they are expressed at the cell surface at levels that are 10−30 times greater than the number of binding sites on cells expressing chromosomally encoded normal full-length Ste2p[74,88] (see Table 2). Thus, the observed defects in signaling by these variants at high temperatures must be due to a loss of receptor signaling function that is not accompanied by loss of ligand binding capabilities.

Decreased abundances of mutant receptors can arise either through a decreased level of synthesis and trafficking or through enhanced unfolding or degradation of receptors. However, no progressive loss of binding sites is seen in variant-expressing cells subjected to short-term treatment at increased temperatures (Figure S6 of the Supporting Information). Thus, the observed decreases in receptor numbers observed upon culturing variant-expressing cells at 34 °C most likely reflect a decreased flux of newly synthesized receptors to the plasma membrane, perhaps caused by recognition and destruction of misfolded proteins by the quality control system of the endoplasmic secretory pathway.[89]

The fact that we observe both increases and decreases in cell-surface abundance in comparisons between full-length and C-terminally truncated temperature-sensitive receptors indicates that two disparate types of effects result from Ste2p truncation. In most cases, C-terminal truncation resulted in increased cell-surface abundances of receptors, as expected if the C-terminal tail is involved in endocytosis and degradation of receptors. However, for one mutation (L211R), C-terminal truncation resulted in decreased numbers of receptors at the cell surface. In such cases, removal of the C-terminal tail may lead to a loss of stabilizing interactions between the C-terminal tail and the rest of the receptor, as has been observed previously for certain mutant forms of Ste2p.[90] Because many constructs used for crystallographic structure determination of GPCRs involve the use of C-terminal truncation to remove portions of the proteins that are expected to be flexible, possible destabilization of receptors by truncation is a factor that merits further consideration.

Mutations That Suppress Temperature Sensitivity. By screening randomly mutagenized temperature-sensitive alleles, we identified 19 intragenic second-site suppressors that result in elevated levels of cell-surface-binding sites for fluorescent ligand. Suppressors that act by providing overall thermodynamic stabilization of receptors would be expected to be "global", meaning that they would be capable of suppressing the effects of multiple temperature-sensitive mutations at different

DOI: 10.1021/bi501314t
Biochemistry 2015, 54, 1787−1806

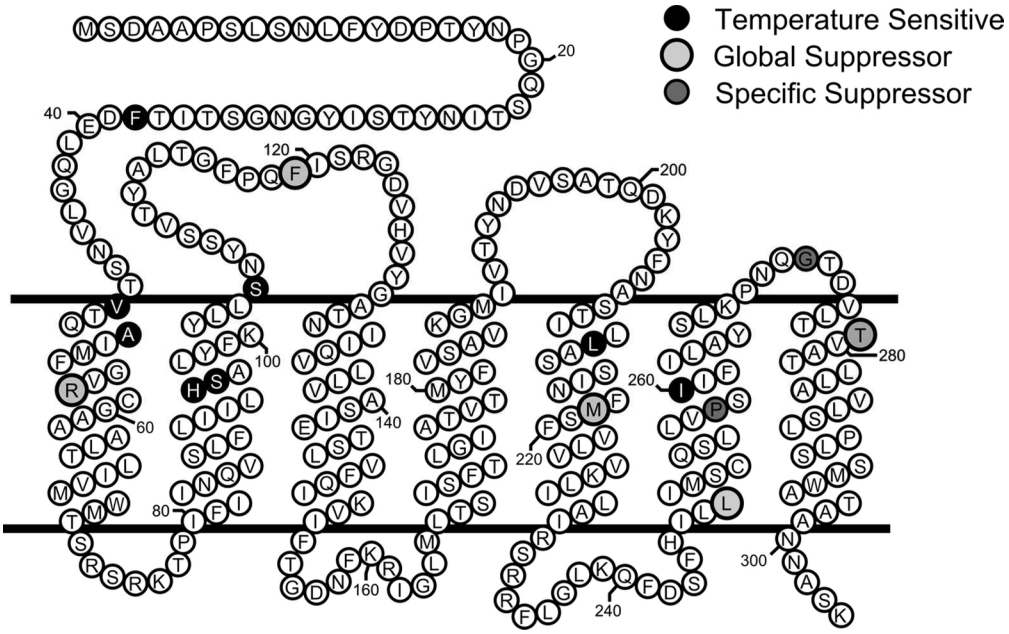

Figure 12. Distribution of suppressor mutations in Ste2p mapped onto the predicted transmembrane topology of Ste2p. The residues with a black background are the locations of the temperature-sensitive mutations. The other highlighted residues indicate the positions of suppressors. Large gray circles show the locations of global suppressors, defined as mutations that restore at least 10% of ligand binding to a 99% confidence level for more than one temperature-sensitive mutation. Residues depicted as smaller dark gray circles are allele-specific suppressors, defined as being able to restore at least 10% of ligand binding to a 99% confidence level for no more than one of the tested temperature-sensitive mutations.

positions in the protein.[65] To examine the full spectrum of interactions between different combinations of suppressors and temperature-sensitive starting alleles, we tested all possible pairings of sets of candidate suppressor and temperature-sensitive mutations to determine numbers of ligand-binding sites at the cell surface after overnight growth at restrictive temperatures (either 30 or 34 °C). Seven mutations (R58G, R58S, F119L, F119S, M218T, L248R, and T279A) of the original 19 candidate suppressors provide "global suppression" in that they are capable of suppressing more than one of the tested temperature-sensitive starting alleles (Figure 7). The locations of these seven suppressor mutations, along with the single-amino acid temperature-sensitive mutations for which suppression was tested, are shown in Figure 12. Both the M218T and the R58G substitutions had been recovered in a prior screen performed by our laboratory, selecting for mutations that suppress the loss-of-signaling function of multiple mutations in the third transmembrane helix of Ste2p.[81] The conclusion that mutations providing global suppression act by providing overall stabilization of the receptor is reinforced by the additive effects seen in combining multiple suppressors with different temperature-sensitive mutations. Enhancements of protein stability achieved by combination of multiple individual stabilizing mutations have been reported for other membrane proteins.[5,51,91]

The suppressor mutations shown in Figure 12 are widely distributed, indicating that determinants of stability are not restricted to one particular region of the sequence. The diversity of the recovered suppressor mutations suggests that stabilizing mutations may be relatively common, implying that there is little evolutionary pressure to maximize Ste2p stability, or even that there may be pressure to maintain instability.[92] Substitutions that enhance stability appear to constitute a common class of mutation in other membrane proteins.[93]

In addition to providing increased numbers of receptors at the cell surface, some of the isolated suppressor mutations, such as substitutions at R58 and F119, also restore enhanced signaling in the growth arrest assay. Suppression of signaling defects of some of the temperature-sensitive starting alleles that result in low cell-surface receptor levels, such as S95Y and S104Y, is likely to be the result of restoration of these levels to the threshold required for effective signal transduction. However, for other temperature-sensitive alleles, such as V49D, that do not greatly reduce numbers of cell-surface-binding sites, suppression must be occurring through a mechanism other than simple augmentation of the numbers of receptors. Instead, the suppressing mutations may be compensating for mechanistic deficiencies in ligand-induced activation of the receptor.

The extent to which the stabilities of membrane proteins in native membranes correspond to stabilities in the detergent-solubilized states of such proteins used for purification and crystallization remains unknown. As an initial step toward characterizing the behavior of potentially stabilized Ste2p variants in detergent, we investigated the antibody-mediated immobilization on polystyrene beads of variants containing suppressor mutations introduced into C-terminally truncated forms of Ste2p. While previous efforts in our laboratory to immobilize and purify truncated Ste2p in the absence of ligand have been unsuccessful, we were able to immobilize the wild-type truncated receptors in the presence of the receptor ligand α-factor, consistent with stabilization of the receptor by ligand[61] and demonstrating that the solubilized receptor remains in a state competent for high-affinity ligand binding. In addition, we were able to achieve immobilization of truncated receptors containing suppressor mutations R58G and R58S even in the absence of ligand, indicating that these mutations can provide stabilization of receptors. (Despite the evidence that solubilized Ste2p retains the capacity for ligand binding, we have not, to

DOI: 10.1021/bi501314t
Biochemistry 2015, 54, 1787−1806

date, been able to directly detect binding of fluorescent ligands to the immobilized receptors under any of the conditions tested. This difficulty stems, in part, from the complications of attempting to determine ligand binding to receptors immobilized in the presence of ligand.)

In addition to the observed patterns of global suppression, several of the identified suppressor mutations exhibit partial specificity for particular temperature-sensitive starting alleles, indicative of specific interactions between the sites of the temperature-sensitive and suppressing mutations. The most striking case of this is the suppression of mutations at several sites on the predicted second transmembrane helix of Ste2p by mutations at R58 in the predicted first transmembrane helix. Mutations at position R58 were unique among the suppressor substitutions in their ability to provide substantial suppression of the temperature-sensitive phenotype of the S95Y substitution. Furthermore, while global suppression of multiple temperature-sensitive mutations was observed only when R58 was replaced with amino acids with small side chains, some specific suppression of S95Y was observed when bulky residues were substituted for R58. This specific suppression may depend on the loss of a positive charge at position 58, because the R58K substitution, which preserves the charge at this position, was the only tested substitution that did not result in significant suppression of S95Y. An additional example of allele-specific suppression involves the temperature-sensitive mutation I260K, which is suppressed by four nearby amino acid substitutions (I256N, P258A, P258L, and G273D) that do not suppress any of the other temperature-sensitive mutations in the tested array (see Figure 7). Substitution of lysine for I260 may result in a distortion of the sixth transmembrane helix that can be reversed by diverse suppressors in this region. This is consistent with previous observations that any replacement of the proline at position 258 (the site of two substitutions that suppress I260K), as well as a variety of other substitutions in neighboring regions of the sixth transmembrane segment, results in constitutive activation of the receptor.[94−96]

In summary, we have developed and tested genetic screens for mutant α-factor receptors that display temperature-sensitive signaling function and temperature-sensitive ligand binding. All of the recovered singly substituted temperature-sensitive alleles exhibit decreases in total and cell-surface expression levels at both low and high temperatures, reflecting either impaired synthesis and targeting or unfolding and degradation by cellular quality control mechanisms. However, temperature sensitivity appears to result from effects on both receptor expression levels and signaling function. We then identified intragenic second-site suppressors of diverse temperature-sensitive alleles from randomly mutagenized libraries, including seven substitutions that were able to suppress multiple temperature-sensitive alleles, indicating that they act by providing overall stabilization of receptors. Detergent-solubilized Ste2p receptors containing substitutions at R58 exhibited improved immobilization onto antibody-conjugated beads and reduced levels of aggregation compared to those of wild-type receptors.

■ ASSOCIATED CONTENT

Supporting Information

Lists of the yeast strains and plasmids used in these studies (Tables S1−S3), summaries of the oligonucleotides used in these studies (Tables S4−S6), a summary of the properties of temperature-sensitive mutations recovered from screening (Table S7), a list of suppressor mutations recovered from screening (Table S8), a representation of the gates used for FACS (Figures S1 and S2), additional assays of α-factor-dependent growth arrest (Figure S3, S7, and S9−S15), additional assays of binding of [K^7(NBD),Nle^{12}]-α-factor to receptors (Figures S4, S5, and S8), assays of the effects of short-term temperature shifts on binding of [K^7(NBD),Nle^{12}]-α-factor to Ste2p receptors (Figure S6), a molecular model of interactions responsible for allele-specific suppression (Figure S16), and immunoblots showing oligomerization of solubilized receptors (Figure S17). This material is available free of charge via the Internet at http://pubs.acs.org.

■ AUTHOR INFORMATION

Corresponding Author

*E-mail: mark_dumont@urmc.rochester.edu. Phone: (585) 275-2466.

Funding

This work was supported by National Institutes of Health Grants R01GM084083 and U54GM09461 to M.E.D. and R01GM22087 to F.N. and American Heart Association Predoctoral Fellowship 0715810T to J.Z.

Notes

The authors declare no competing financial interest.

[§]Leonard and Esther Kurtz Term Professor.

■ ACKNOWLEDGMENTS

We thank Ryan Over for technical assistance and Elizabeth Grayhack, Patricia Hinkle, and Eric Phizicky for invaluable discussions. Flow cytometry and fluorescence-activated cell sorting were performed using the facilities of the University of Rochester Flow Cytometry Core Facility.

■ ABBREVIATIONS

TMP, transmembrane protein; GPCR, G protein-coupled receptor; NBD, 7-nitrobenz-2-oxa-1,3-diazol-4-yl; FACS, fluorescence-activated cell sorting.

■ REFERENCES

(1) Wallin, E., and Heijne, G. V. (1998) Genome-wide analysis of integral membrane proteins from eubacterial, archaean, and eukaryotic organisms. *Protein Sci. 7*, 1029−1038.

(2) Overington, J. P., Al-Lazikani, B., and Hopkins, A. L. (2006) How many drug targets are there? *Nat. Rev. Drug Discovery 5*, 993−996.

(3) White, S. H. (2009) Biophysical dissection of membrane proteins. *Nature 459*, 344−346.

(4) Lundstrom, K. (2005) Structural biology of G protein-coupled receptors. *Bioorg. Med. Chem. Lett. 15*, 3654−3657.

(5) Miller, J. L., and Tate, C. G. (2011) Engineering an Ultra-Thermostable β1-Adrenoceptor. *J. Mol. Biol. 413*, 628−638.

(6) Sonoda, Y., Newstead, S., Hu, N. J., Alguel, Y., Nji, E., Beis, K., Yashiro, S., Lee, C., Leung, J., Cameron, A. D., Byrne, B., Iwata, S., and Drew, D. (2011) Benchmarking membrane protein detergent stability for improving throughput of high-resolution X-ray structures. *Structure 19*, 17−25.

(7) Jiang, Y., Lee, A., Chen, J., Ruta, V., Cadene, M., Chait, B. T., and MacKinnon, R. (2003) X-ray structure of a voltage-dependent K$^+$ channel. *Nature 423*, 33−41.

(8) Chun, E., Thompson, A. A., Liu, W., Roth, C. B., Griffith, M. T., Katritch, V., Kunken, J., Xu, F., Cherezov, V., Hanson, M. A., and Stevens, R. C. (2012) Fusion partner toolchest for the stabilization and crystallization of G protein-coupled receptors. *Structure 20*, 967−976.

(9) Rosenbaum, D. M., Cherezov, V., Hanson, M. A., Rasmussen, S. G. F., Thian, F. S., Kobilka, T. S., Choi, H.-J., Yao, X.-J., Weis, W. I., Stevens, R. C., and Kobilka, B. K. (2007) GPCR Engineering Yields

DOI: 10.1021/bi501314t
Biochemistry 2015, 54, 1787−1806

High-Resolution Structural Insights into β2-Adrenergic Receptor Function. *Science 318*, 1266−1273.
(10) Cherezov, V., Rosenbaum, D. M., Hanson, M. A., Rasmussen, S. G. F., Thian, F. S., Kobilka, T. S., Choi, H.-J., Kuhn, P., Weis, W. I., Kobilka, B. K., and Stevens, R. C. (2007) High-Resolution Crystal Structure of an Engineered Human β2-Adrenergic G Protein Coupled Receptor. *Science 318*, 1258−1265.
(11) Jaakola, V.-P., Griffith, M. T., Hanson, M. A., Cherezov, V., Chien, E. Y. T., Lane, J. R., Ijzerman, A. P., and Stevens, R. C. (2008) The 2.6 Angstrom Crystal Structure of a Human A2A Adenosine Receptor Bound to an Antagonist. *Science 322*, 1211−1217.
(12) Wu, B., Chien, E. Y. T., Mol, C. D., Fenalti, G., Liu, W., Katritch, V., Abagyan, R., Brooun, A., Wells, P., Bi, F. C., Hamel, D. J., Kuhn, P., Handel, T. M., Cherezov, V., and Stevens, R. C. (2010) Structures of the CXCR4 Chemokine GPCR with Small-Molecule and Cyclic Peptide Antagonists. *Science 330*, 1066−1071.
(13) Chien, E. Y. T., Liu, W., Zhao, Q., Katritch, V., Won Han, G., Hanson, M. A., Shi, L., Newman, A. H., Javitch, J. A., Cherezov, V., and Stevens, R. C. (2010) Structure of the Human Dopamine D3 Receptor in Complex with a D2/D3 Selective Antagonist. *Science 330*, 1091−1095.
(14) Xu, F., Wu, H., Katritch, V., Han, G. W., Jacobson, K. A., Gao, Z.-G., Cherezov, V., and Stevens, R. C. (2011) Structure of an Agonist-Bound Human A2A Adenosine Receptor. *Science 332*, 322−327.
(15) Rosenbaum, D. M., Zhang, C., Lyons, J. A., Holl, R., Aragao, D., Arlow, D. H., Rasmussen, S. G. F., Choi, H.-J., DeVree, B. T., Sunahara, R. K., Chae, P. S., Gellman, S. H., Dror, R. O., Shaw, D. E., Weis, W. I., Caffrey, M., Gmeiner, P., and Kobilka, B. K. (2011) Structure and function of an irreversible agonist-[bgr]2 adrenoceptor complex. *Nature 469*, 236−240.
(16) Rasmussen, S. G. F., Choi, H.-J., Fung, J. J., Pardon, E., Casarosa, P., Chae, P. S., DeVree, B. T., Rosenbaum, D. M., Thian, F. S., Kobilka, T. S., Schnapp, A., Konetzki, I., Sunahara, R. K., Gellman, S. H., Pautsch, A., Steyaert, J., Weis, W. I., and Kobilka, B. K. (2011) Structure of a nanobody-stabilized active state of the [bgr]2 adrenoceptor. *Nature 469*, 175−180.
(17) Rasmussen, S. G. F., DeVree, B. T., Zou, Y., Kruse, A. C., Chung, K. Y., Kobilka, T. S., Thian, F. S., Chae, P. S., Pardon, E., Calinski, D., Mathiesen, J. M., Shah, S. T. A., Lyons, J. A., Caffrey, M., Gellman, S. H., Steyaert, J., Skiniotis, G., Weis, W. I., Sunahara, R. K., and Kobilka, B. K. (2011) Crystal structure of the [**bgr**]2 adrenergic receptor-Gs protein complex. *Nature 477*, 549−555.
(18) Shimamura, T., Shiroishi, M., Weyand, S., Tsujimoto, H., Winter, G., Katritch, V., Abagyan, R., Cherezov, V., Liu, W., Han, G. W., Kobayashi, T., Stevens, R. C., and Iwata, S. (2011) Structure of the human histamine H1 receptor complex with doxepin. *Nature 475*, 65−70.
(19) Granier, S., Manglik, A., Kruse, A. C., Kobilka, T. S., Thian, F. S., Weis, W. I., and Kobilka, B. K. (2012) Structure of the δ-opioid receptor bound to naltrindole. *Nature 485*, 400−404.
(20) Wu, H., Wacker, D., Mileni, M., Katritch, V., Han, G. W., Vardy, E., Liu, W., Thompson, A. A., Huang, X.-P., Carroll, F. I., Mascarella, S. W., Westkaemper, R. B., Mosier, P. D., Roth, B. L., Cherezov, V., and Stevens, R. C. (2012) Structure of the human κ-opioid receptor in complex with JDTic. *Nature 485*, 327−332.
(21) Manglik, A., Kruse, A. C., Kobilka, T. S., Thian, F. S., Mathiesen, J. M., Sunahara, R. K., Pardo, L., Weis, W. I., Kobilka, B. K., and Granier, S. (2012) Crystal structure of the μ-opioid receptor bound to a morphinan antagonist. *Nature 485*, 321−326.
(22) Haga, K., Kruse, A. C., Asada, H., Yurugi-Kobayashi, T., Shiroishi, M., Zhang, C., Weis, W. I., Okada, T., Kobilka, B. K., Haga, T., and Kobayashi, T. (2012) Structure of the human M2 muscarinic acetylcholine receptor bound to an antagonist. *Nature 482*, 547−551.
(23) Kruse, A. C., Hu, J., Pan, A. C., Arlow, D. H., Rosenbaum, D. M., Rosemond, E., Green, H. F., Liu, T., Chae, P. S., Dror, R. O., Shaw, D. E., Weis, W. I., Wess, J., and Kobilka, B. K. (2012) Structure and dynamics of the M3 muscarinic acetylcholine receptor. *Nature 482*, 552−556.
(24) White, J. F., Noinaj, N., Shibata, Y., Love, J., Kloss, B., Xu, F., Gvozdenovic-Jeremic, J., Shah, P., Shiloach, J., Tate, C. G., and Grisshammer, R. (2012) Structure of the agonist-bound neurotensin receptor. *Nature 490*, 508−513.
(25) Zhang, C., Srinivasan, Y., Arlow, D. H., Fung, J. J., Palmer, D., Zheng, Y., Green, H. F., Pandey, A., Dror, R. O., Shaw, D. E., Weis, W. I., Coughlin, S. R., and Kobilka, B. K. (2012) High-resolution crystal structure of human protease-activated receptor 1. *Nature 492*, 387−392.
(26) Hanson, M. A., Roth, C. B., Jo, E., Griffith, M. T., Scott, F. L., Reinhart, G., Desale, H., Clemons, B., Cahalan, S. M., Schuerer, S. C., Sanna, M. G., Han, G. W., Kuhn, P., Rosen, H., and Stevens, R. C. (2012) Crystal Structure of a Lipid G Protein-Coupled Receptor. *Science 335*, 851−855.
(27) Thompson, A. A., Liu, W., Chun, E., Katritch, V., Wu, H., Vardy, E., Huang, X.-P., Trapella, C., Guerrini, R., Calo, G., Roth, B. L., Cherezov, V., and Stevens, R. C. (2012) Structure of the nociceptin/orphanin FQ receptor in complex with a peptide mimetic. *Nature 485*, 395−399.
(28) Hollenstein, K., Kean, J., Bortolato, A., Cheng, R. K., Dore, A. S., Jazayeri, A., Cooke, R. M., Weir, M., and Marshall, F. H. (2013) Structure of class B GPCR corticotropin-releasing factor receptor 1. *Nature 499*, 438−443.
(29) Wang, C., Jiang, Y., Ma, J., Wu, H., Wacker, D., Katritch, V., Han, G. W., Liu, W., Huang, X.-P., Vardy, E., McCorvy, J. D., Gao, X., Zhou, X. E., Melcher, K., Zhang, C., Bai, F., Yang, H., Yang, L., Jiang, H., Roth, B. L., Cherezov, V., Stevens, R. C., and Xu, H. E. (2013) Structural Basis for Molecular Recognition at Serotonin Receptors. *Science 340*, 610−614.
(30) Wang, C., Wu, H., Katritch, V., Han, G. W., Huang, X. P., Liu, W., Siu, F. Y., Roth, B. L., Cherezov, V., and Stevens, R. C. (2013) Structure of the human smoothened receptor bound to an antitumour agent. *Nature 497*, 338−343.
(31) Wacker, D., Wang, C., Katritch, V., Han, G. W., Huang, X.-P., Vardy, E., McCorvy, J. D., Jiang, Y., Chu, M., Siu, F. Y., Liu, W., Xu, H. E., Cherezov, V., Roth, B. L., and Stevens, R. C. (2013) Structural Features for Functional Selectivity at Serotonin Receptors. *Science 340*, 615−619.
(32) Siu, F. Y., He, M., de Graaf, C., Han, G. W., Yang, D., Zhang, Z., Zhou, C., Xu, Q., Wacker, D., Joseph, J. S., Liu, W., Lau, J., Cherezov, V., Katritch, V., Wang, M. W., and Stevens, R. C. (2013) Structure of the human glucagon class B G-protein-coupled receptor. *Nature 499*, 444−449.
(33) Tan, Q., Zhu, Y., Li, J., Chen, Z., Han, G. W., Kufareva, I., Li, T., Ma, L., Fenalti, G., Li, J., Zhang, W., Xie, X., Yang, H., Jiang, H., Cherezov, V., Liu, H., Stevens, R. C., Zhao, Q., and Wu, B. (2013) Structure of the CCR5 chemokine receptor-HIV entry inhibitor maraviroc complex. *Science 341*, 1387−1390.
(34) Fenalti, G., Giguere, P. M., Katritch, V., Huang, X. P., Thompson, A. A., Cherezov, V., Roth, B. L., and Stevens, R. C. (2014) Molecular control of δ-opioid receptor signalling. *Nature 506*, 191−196.
(35) Dore, A. S., Okrasa, K., Patel, J. C., Serrano-Vega, M., Bennett, K., Cooke, R. M., Errey, J. C., Jazayeri, A., Khan, S., Tehan, B., Weir, M., Wiggin, G. R., and Marshall, F. H. (2014) Structure of class C GPCR metabotropic glutamate receptor 5 transmembrane domain. *Nature 511*, 557−562.
(36) Wu, H., Wang, C., Gregory, K. J., Han, G. W., Cho, H. P., Xia, Y., Niswender, C. M., Katritch, V., Meiler, J., Cherezov, V., Conn, P. J., and Stevens, R. C. (2014) Structure of a class C GPCR metabotropic glutamate receptor 1 bound to an allosteric modulator. *Science 344*, 58−64.
(37) Zhang, J., Zhang, K., Gao, Z. G., Paoletta, S., Zhang, D., Han, G. W., Li, T., Ma, L., Zhang, W., Muller, C. E., Yang, H., Jiang, H., Cherezov, V., Katritch, V., Jacobson, K. A., Stevens, R. C., Wu, B., and Zhao, Q. (2014) Agonist-bound structure of the human P2Y12 receptor. *Nature 509*, 119−122.
(38) Zhang, K., Zhang, J., Gao, Z. G., Zhang, D., Zhu, L., Han, G. W., Moss, S. M., Paoletta, S., Kiselev, E., Lu, W., Fenalti, G., Zhang, W.,

DOI: 10.1021/bi501314t
Biochemistry 2015, 54, 1787−1806

Muller, C. E., Yang, H., Jiang, H., Cherezov, V., Katritch, V., Jacobson, K. A., Stevens, R. C., Wu, B., and Zhao, Q. (2014) Structure of the human P2Y12 receptor in complex with an antithrombotic drug. *Nature 509*, 115−118.
(39) Tate, C. G. (2012) A crystal clear solution for determining G-protein-coupled receptor structures. *Trends Biochem. Sci. 37*, 343−352.
(40) Warne, T., Serrano-Vega, M. J., Baker, J. G., Moukhametzianov, R., Edwards, P. C., Henderson, R., Leslie, A. G. W., Tate, C. G., and Schertler, G. F. X. (2008) Structure of a [bgr]1-adrenergic G-protein-coupled receptor. *Nature 454*, 486−491.
(41) Doré, A. S., Robertson, N., Errey, J. C., Ng, I., Hollenstein, K., Tehan, B., Hurrell, E., Bennett, K., Congreve, M., Magnani, F., Tate, C. G., Weir, M., and Marshall, F. H. (2011) Structure of the Adenosine A2A Receptor in Complex with ZM241385 and the Xanthines XAC and Caffeine. *Structure 19*, 1283−1293.
(42) Lebon, G., Warne, T., Edwards, P. C., Bennett, K., Langmead, C. J., Leslie, A. G. W., and Tate, C. G. (2011) Agonist-bound adenosine A2A receptor structures reveal common features of GPCR activation. *Nature 474*, 521−525.
(43) Warne, T., Moukhametzianov, R., Baker, J. G., Nehmé, R., Edwards, P. C., Leslie, A. G. W., Schertler, G. F. X., and Tate, C. G. (2011) The structural basis for agonist and partial agonist action on a β1-adrenergic receptor. *Nature 469*, 241−244.
(44) Warne, T., Edwards, P. C., Leslie, A. G. W., and Tate, C. G. (2012) Crystal Structures of a Stabilized β1-Adrenoceptor Bound to the Biased Agonists Bucindolol and Carvedilol. *Structure 20*, 841−849.
(45) Egloff, P., Hillenbrand, M., Klenk, C., Batyuk, A., Heine, P., Balada, S., Schlinkmann, K. M., Scott, D. J., Schutz, M., and Pluckthun, A. (2014) Structure of signaling-competent neurotensin receptor 1 obtained by directed evolution in *Escherichia coli*. *Proc. Natl. Acad. Sci. U.S.A. 111*, E655−E662.
(46) Hunte, C., and Michel, H. (2002) Crystallisation of membrane proteins mediated by antibody fragments. *Curr. Opin. Struct. Biol. 12*, 503−508.
(47) Rasmussen, S. G. F., Choi, H.-J., Rosenbaum, D. M., Kobilka, T. S., Thian, F. S., Edwards, P. C., Burghammer, M., Ratnala, V. R. P., Sanishvili, R., Fischetti, R. F., Schertler, G. F. X., Weis, W. I., and Kobilka, B. K. (2007) Crystal structure of the human β2 adrenergic G-protein-coupled receptor. *Nature 450*, 383−387.
(48) Kohl, A., Binz, H. K., Forrer, P., Stumpp, M. T., Plückthun, A., and Grütter, M. G. (2003) Designed to be stable: Crystal structure of a consensus ankyrin repeat protein. *Proc. Natl. Acad. Sci. U.S.A. 100*, 1700−1705.
(49) Dodevski, I., and Plückthun, A. (2011) Evolution of Three Human GPCRs for Higher Expression and Stability. *J. Mol. Biol. 408*, 599−615.
(50) Sarkar, C. A., Dodevski, I., Kenig, M., Dudli, S., Mohr, A., Hermans, E., and Plückthun, A. (2008) Directed evolution of a G protein-coupled receptor for expression, stability, and binding selectivity. *Proc. Natl. Acad. Sci. U.S.A. 105*, 14808−14813.
(51) Schlinkmann, K. M., Hillenbrand, M., Rittner, A., Künz, M., Strohner, R., and Plückthun, A. (2012) Maximizing Detergent Stability and Functional Expression of a GPCR by Exhaustive Recombination and Evolution. *J. Mol. Biol. 422*, 414−428.
(52) Schlinkmann, K. M., Honegger, A., Türeci, E., Robison, K. E., Lipovšek, D., and Plückthun, A. (2012) Critical features for biosynthesis, stability, and functionality of a G protein-coupled receptor uncovered by all-versus-all mutations. *Proc. Natl. Acad. Sci. U.S.A. 109*, 9810−9815.
(53) Scott, D. J., Kummer, L., Tremmel, D., and Plückthun, A. (2013) Stabilizing membrane proteins through protein engineering. *Curr. Opin. Chem. Biol. 17*, 427−435.
(54) Scott, D. J., and Plückthun, A. (2013) Direct Molecular Evolution of Detergent-Stable G Protein-Coupled Receptors Using Polymer Encapsulated Cells. *J. Mol. Biol. 425*, 662−677.
(55) Palczewski, K., Kumasaka, T., Hori, T., Behnke, C. A., Motoshima, H., Fox, B. A., Trong, I. L., Teller, D. C., Okada, T., Stenkamp, R. E., Yamamoto, M., and Miyano, M. (2000) Crystal Structure of Rhodopsin: A G Protein-Coupled Receptor. *Science 289*, 739−745.
(56) Serrano-Vega, M. J., Magnani, F., Shibata, Y., and Tate, C. G. (2008) Conformational thermostabilization of the β1-adrenergic receptor in a detergent-resistant form. *Proc. Natl. Acad. Sci. U.S.A. 105*, 877−882.
(57) Leberer, E., Dignard, D., Harcus, D., Thomas, D. Y., and Whiteway, M. (1992) The protein kinase homologue Ste20p is required to link the yeast pheromone response G-protein $\beta\gamma$ subunits to downstream signalling components. *EMBO J. 11*, 4815−4824.
(58) Price, L. A., Kajkowski, E. M., Hadcock, J. R., Ozenberger, B. A., and Pausch, M. H. (1995) Functional coupling of a mammalian somatostatin receptor to the yeast pheromone response pathway. *Mol. Cell. Biol. 15*, 6188−6195.
(59) King, K., Dohlman, H. G., Thorner, J., Caron, M. G., and Lefkowitz, R. J. (1990) Control of yeast mating signal transduction by a mammalian β2-adrenergic receptor and Gs α subunit. *Science 250*, 121−123.
(60) Brown, A. J., Dyos, S. L., Whiteway, M. S., White, J. H. M., Watson, M.-A. E. A., Marzioch, M., Clare, J. J., Cousens, D. J., Paddon, C., Plumpton, C., Romanos, M. A., and Dowell, S. J. (2000) Functional coupling of mammalian receptors to the yeast mating pathway using novel yeast/mammalian G protein α-subunit chimeras. *Yeast 16*, 11−22.
(61) David, N. E., Gee, M., Andersen, B., Naider, F., Thorner, J., and Stevens, R. C. (1997) Expression and Purification of the *Saccharomyces cerevisiae* α-Factor Receptor (Ste2p), a 7-Transmembrane-segment G Protein-coupled Receptor. *J. Biol. Chem. 272*, 15553−15561.
(62) Lee, B. K., Jung, K. S., Son, C., Kim, H., VerBerkmoes, N. C., Arshava, B., Naider, F., and Becker, J. M. (2007) Affinity purification and characterization of a G-protein coupled receptor, *Saccharomyces cerevisiae* Ste2p. *Protein Expression Purif. 56*, 62−71.
(63) Shi, C., Shin, Y.-O., Hanson, J., Cass, B., Loewen, M. C., and Durocher, Y. (2005) Purification and Characterization of a Recombinant G-Protein-Coupled Receptor, *Saccharomyces cerevisiae* Ste2p, Transiently Expressed in HEK293 EBNA1 Cells. *Biochemistry 44*, 15705−15714.
(64) Jenness, D. D., Li, Y., Tipper, C., and Spatrick, P. (1997) Elimination of defective α-factor pheromone receptors. *Mol. Cell. Biol. 17*, 6236−6245.
(65) Shortle, D., and Lin, B. (1985) Genetic Analysis of Staphylococcal Nuclease: Identification of Three Intragenic "global" Suppressors of Nuclease-Minus Mutations. *Genetics 110*, 539−555.
(66) Leavitt, L. M., Macaluso, C. R., Kim, K. S., Martin, N. P., and Dumont, M. E. (1999) Dominant negative mutations in the α-factor receptor, a G protein-coupled receptor encoded by the STE2 gene of the yeast *Saccharomyces cerevisiae*. *Mol. Gen. Genet. 261*, 917−932.
(67) Jenness, D. D., Goldman, B. S., and Hartwell, L. H. (1987) *Saccharomyces cerevisiae* mutants unresponsive to α-factor pheromone: α-Factor binding and extragenic suppression. *Mol. Cell. Biol. 7*, 1311−1319.
(68) Gehret, A. U., Connelly, S. M., and Dumont, M. E. (2012) Functional and Physical Interactions among *Saccharomyces cerevisiae* α-Factor Receptors. *Eukaryotic Cell 11*, 1276−1288.
(69) Tantry, S., Ding, F.-X., Dumont, M., Becker, J. M., and Naider, F. (2010) Binding of Fluorinated Phenylalanine α-Factor Analogues to Ste2p: Evidence for a Cation−π Binding Interaction between a Peptide Ligand and Its Cognate G Protein-Coupled Receptor. *Biochemistry 49*, 5007−5015.
(70) Kunkel, T. A. (1985) Rapid and efficient site-specific mutagenesis without phenotypic selection. *Proc. Natl. Acad. Sci. U.S.A. 82*, 488−492.
(71) Celic, A., Connelly, S. M., Martin, N. P., and Dumont, M. E. (2004) Intensive mutational analysis of G protein-coupled receptors in yeast. *Methods Mol. Biol. 237*, 105−120.
(72) Sommers, C. M., and Dumont, M. E. (1999) *Genetic approaches for studying the structure and function of G protein-coupled receptors in yeast*, Wiley-Liss, New York.

DOI: 10.1021/bi501314t
Biochemistry 2015, 54, 1787−1806

(73) Ding, F.-X., Lee, B. K., Hauser, M., Davenport, L., Becker, J. M., and Naider, F. (2001) Probing the Binding Domain of the *Saccharomyces cerevisiae* α-Mating Factor Receptor with Fluorescent Ligands. *Biochemistry 40*, 1102−1108.
(74) Bajaj, A., Ćelić, A., Ding, F.-X., Naider, F., Becker, J. M., and Dumont, M. E. (2004) A Fluorescent α-Factor Analogue Exhibits Multiple Steps on Binding to Its G Protein Coupled Receptor in Yeast. *Biochemistry 43*, 13564−13578.
(75) Taslimi, A., Mathew, E., Ćelić, A., Wessel, S., and Dumont, M. E. (2012) Identifying Functionally Important Conformational Changes in Proteins: Activation of the Yeast α-factor Receptor Ste2p. *J. Mol. Biol. 418*, 367−378.
(76) Li, Y., Kane, T., Tipper, C., Spatrick, P., and Jenness, D. D. (1999) Yeast Mutants Affecting Possible Quality Control of Plasma Membrane Proteins. *Mol. Cell. Biol. 19*, 3588−3599.
(77) Rasse-Messenguy, F., and Fink, G. R. (1973) Temperature-sensitive nonsense suppressors in yeast. *Genetics 75*, 459−464.
(78) Konopka, J. B., Jenness, D. D., and Hartwell, L. H. (1988) The C-terminus of the *S. cerevisiae* α-pheromone receptor mediates an adaptive response to pheromone. *Cell 54*, 609−620.
(79) Reneke, J. E., Blumer, K. J., Courchesne, W. E., and Thorner, J. (1988) The carboxy-terminal segment of the yeast α-factor receptor is a regulatory domain. *Cell 55*, 221−234.
(80) Shah, A., and Marsh, L. (1996) Role of Sst2 in modulating G protein-coupled receptor signaling. *Biochem. Biophys. Res. Commun. 226*, 242−246.
(81) Sommers, C. M., and Dumont, M. E. (1997) Genetic interactions among the transmembrane segments of the G protein coupled receptor encoded by the yeast STE2 gene. *J. Mol. Biol. 266*, 559−575.
(82) Eilers, M., Hornak, V., Smith, S. O., and Konopka, J. B. (2005) Comparison of Class A and D G Protein-Coupled Receptors: Common Features in Structure and Activation. *Biochemistry 44*, 8959−8975.
(83) Son, C. D., Sargsyan, H., Naider, F., and Becker, J. M. (2004) Identification of ligand binding regions of the *Saccharomyces cerevisiae* α-factor pheromone receptor by photoaffinity cross-linking. *Biochemistry 43*, 13193−13203.
(84) Umanah, G. K., Son, C., Ding, F., Naider, F., and Becker, J. M. (2009) Cross-linking of a DOPA-containing peptide ligand into its G protein-coupled receptor. *Biochemistry 48*, 2033−2044.
(85) White, M. A., Clark, K. M., Grayhack, E. J., and Dumont, M. E. (2007) Characteristics Affecting Expression and Solubilization of Yeast Membrane Proteins. *J. Mol. Biol. 365*, 621−636.
(86) Mentesana, P. E., and Konopka, J. B. (2001) Mutational analysis of the role of N-glycosylation in α-factor receptor function. *Biochemistry 40*, 9685−9694.
(87) Serrano-Vega, M. J., and Tate, C. G. (2009) Transferability of thermostabilizing mutations between β-adrenergic receptors. *Mol. Membr. Biol. 26*, 385−396.
(88) Gehret, A. U., Bajaj, A., Naider, F., and Dumont, M. E. (2006) Oligomerization of the Yeast α-Factor Receptor. *J. Biol. Chem. 281*, 20698−20714.
(89) Brodsky, J. L., and Skach, W. R. (2011) Protein folding and quality control in the endoplasmic reticulum: Recent lessons from yeast and mammalian cell systems. *Curr. Opin. Cell Biol. 23*, 464−475.
(90) Mathew, E., Ding, F.-X., Naider, F., and Dumont, M. E. (2013) Functional fusions of T4 lysozyme in the third intracellular loop of a G protein-coupled receptor identified by a random screening approach in yeast. *Protein Eng., Des. Sel. 26*, 59−71.
(91) Lebon, G., Bennett, K., Jazayeri, A., and Tate, C. G. (2011) Thermostabilisation of an agonist-bound conformation of the human adenosine A(2A) receptor. *J. Mol. Biol. 409*, 298−310.
(92) Hong, H., and Bowie, J. U. (2011) Dramatic destabilization of transmembrane helix interactions by features of natural membrane environments. *J. Am. Chem. Soc. 133*, 11389−11398.
(93) Bowie, J. U. (2001) Stabilizing membrane proteins. *Curr. Opin. Struct. Biol. 11*, 397−402.
(94) Konopka, J. B., Margarit, S. M., and Dube, P. (1996) Mutation of Pro-258 in transmembrane domain 6 constitutively activates the G protein-coupled α-factor receptor. *Proc. Natl. Acad. Sci. U.S.A. 93*, 6764−6769.
(95) Sommers, C. M., Martin, N. P., Akal-Strader, A., Becker, J. M., Naider, F., and Dumont, M. E. (2000) A Limited Spectrum of Mutations Causes Constitutive Activation of the Yeast α-Factor Receptor. *Biochemistry 39*, 6898−6909.
(96) Stefan, C. J., Overton, M. C., and Blumer, K. J. (1998) Mechanisms Governing the Activation and Trafficking of Yeast G Protein-coupled Receptors. *Mol. Biol. Cell 9*, 885−899.

DOI: 10.1021/bi501314t
Biochemistry 2015, 54, 1787−1806